

Chapter 3

Models and Finite Elements for Thin-walled Structures

M. Bischoff¹, W. A. Wall², K.-U. Bletzinger¹ and E. Ramm³

¹Lehrstuhl für Statik, TU München, München, Germany

²Lehrstuhl für Numerische Mechanik, TU München, Garching, Germany

³Institut für Baustatik, Universität Stuttgart, Stuttgart, Germany

1 Introduction	1
2 Mathematical and Mechanical Foundations	5
3 Plates and Shells	10
4 Dimensional Reduction and Structural Models	12
5 Finite Element Formulation	50
6 Concluding Remarks	70
7 Related Chapters	71
Acknowledgments	71
References	71
Further Reading	75
Appendix	76

1 INTRODUCTION

1.1 Historical remarks

Thin-walled structures like plates and shells are the most common construction elements in nature and technology. This is independent of the specific scale; they might be small like cell membranes and tiny machine parts or very large like fuselages and cooling towers. This preference to

apply walls as thin as possible is a natural optimization strategy to reduce dead load and to minimize construction material. In addition to the slenderness, the advantageous effect of curvature is utilized in shell structures allowing to carry transverse loading in an optimal way, a design principle already known to the ancient master builders. Their considerable heuristic knowledge allowed them to create remarkable buildings, like the Roman Pantheon (115–126) and the Hagia Sophia (532–537) in Constantinople, still existing today. It was not before the Renaissance that scientists began to mathematically idealize the structural response, a process that we denote nowadays as modeling and simulation.

Already, Leonardo da Vinci (1452–1519) stated (Codex Madrid I) a principle that later on emerged to a *beam* model. The subsequent process, associated with names like Galileo (1564–1642), Mariotte (1620–1684), Leibniz (1646–1716), Jakob I Bernoulli (1654–1705), Euler (1707–1783), Coulomb (1736–1806), and Navier (1785–1836), led to what we call today Euler–Bernoulli beam theory (Timoshenko, 1953; Szabo, 1979). This development was driven by the ingenious ideas to condense the complex three-dimensional situation to the essential ingredients of structural response like stretching, bending, torsion, and so on, and to cast this into a manageable mathematical format. The inclusion of transverse shear deformation is attributed (1859) to Bresse (1822–1883) and extended (1921) to dynamics by Timoshenko (1878–1972), whose name has established itself as a common denomination for this model. Extensions to further effects like uniform and warping torsion, stability problems,

cross-sectional distortion, and further refinements, for example, including higher-order kinematics, follows in the nineteenth and twentieth century.

The development of the theory of masonry arches and vaults had its own history, also starting with Leonardo da Vinci (for a detailed elaboration on this subject confer (Benvenuto, 1991)). The primary aspect in this context was the description of failure mechanisms, a problem investigated up to the present time (see e.g. the valuable work of Heyman). Also, Robert Hooke's (1635–1703) 'Riddle of the Arch' has to be referred to, phrased in a Latin anagram 'Ut pendet continuum flexile, sic stabit contiguum inversum rigidum' (literally translated: As the flexible cable hangs, the inverted arch stands). It constitutes a form-finding principle for arches and shells (Mainstone, 1975), which became known as the inverted chain and membrane principle, often applied in the sequel. Christopher Wren's construction of St. Paul Cathedral in London, Poleni's experiment for the rehabilitation of the cupola of St. Peter in Rome, Rondelet's French Pantheon, Gaudi's work in Catalonia up to modern shell designs by Otto and Isler are based on this principle (Ramm and Reiting, 1992).

The history of the development of two-dimensional *plate* theories has its own peculiarities (Timoshenko, 1953; Szabo, 1979). Inspired by Chladni's (1756–1827) experiments with vibrating plates, Jakob II Bernoulli (1759–1789) formulated a grid model of overlapping beams, neglecting the twisting mode. This was corrected by others later on. The related competition proposed by the French Academy and Sophie Germain's (1776–1831) various trials to win the prize and the involvement of Lagrange (1736–1813) became famous. They and others like Poisson (1781–1840) and Navier derived the proper differential equation; however, they still had some shortcomings in their result, in particular, with respect to the involved elastic constants. Kirchhoff (1824–1887) finally removed all doubts in 1850 (Kirchhoff, 1850) and is credited as the founder of modern plate theory. It took almost a century before E. Reissner (1913–1996) (Reissner, 1944; Reissner, 1945) and Mindlin (1906–1987) (Mindlin, 1951) extended the model including the role of transverse shear deformations. Innumerable modifications and extensions, like anisotropy, large deformation (v. Kármán plate theory), higher-order theories, and so on, have been derived over the years.

It is interesting that the initial derivation of a *shell* formulation was also motivated primarily by vibration problems. Euler developed in 1764 a model to simulate the tones of bells, cutting the axisymmetric structure into rings, applying curved beam models and leaving out the meridional effects. Also, here it took over a century before a consistent theory of thin shells had been derived by Love (1888) (August E. H. Love, 1863–1940). It is based on Kirchhoff's method

and thus became known as the Kirchhoff–Love model. For a description of the subsequent emergence of this shell model and the related controversies among Love and his contemporaries on the role of the boundary conditions of both the membrane and the bending part (in particular Lord Rayleigh (1842–1919) and Lamb (1849–1934)), we refer to the article by Calladine (1988), which is worth reading. The need for detailed solutions has driven research in the first half of the twentieth century. Names like H. Reissner, Meissner, Geckeler, Flügge, Vlassov, Novozhilov have to be mentioned, to name just a few; later on further refinements have been introduced by E. Reissner, Gol'denveizer, Koiter, Naghdi, and many others. The inclusion of transverse shear deformations sometimes linked to the name of Naghdi today mostly is referred to as a Reissner–Mindlin formulation, in recognition of their extended plate theories.

The series of names in connection with shell formulations could be continued forever; there are very few topics in structural mechanics where so many investigations have been published. Even for experts, it is hardly possible to have an overall view on the number of special finite element models developed so far. This is a strong indication for the complexity of the involved mechanics on the one hand and their practical relevance on the other hand.

It is obvious that the early developments of theories for thin-walled structures were governed primarily by the main applications in those times, namely, buildings in architecture. Since the industrial revolution, the picture changed completely: now other applications, for example, in mechanical engineering, in vehicle and aerospace industry, in biomechanics, and so on, became dominant and the driving force for further developments.

Large displacements, rotations and strains, buckling, composites, material nonlinearities, coupled problems, multiscale and multiphysics, solution methods, and higher-order formulations are a few keywords for problems that have been extensively investigated in the last few years. The finite element method as a discretization concept is absolutely predominant. An interesting example as to how the finite element developments have influenced the selection of specific structural models is the early shift from Kirchhoff–Love formulations to those with Reissner–Mindlin kinematics for plate and shell elements. It is motivated mainly by the reduced compatibility requirements, although from the practical point of application, the Kirchhoff–Love model is often sufficient.

In times where computer capacity has become so powerful and the simulation tools have reached such a high level of sophistication, we should not forget the main driving force of our ancestors: concentration on the essentials and reduction to the principal mechanical behavior of thin-walled structures (Ramm and Wall, 2004).

1.2 Overview

This paper concentrates on the mathematical modeling of nonlinear mechanics of thin-walled structures in view of associated finite element formulations. This means that we will primarily focus on formulations for structural models as prerequisite for derivation of finite elements, rather than specific ‘elementology’. The main emphasis is put on shells, including the special case of flat plates, turning into shells anyway in the nonlinear regime. The derivations are kept as general as possible, including thick and layered shells (laminated or sandwich structures), as well as anisotropic and inhomogeneous materials from the outset. Throughout Section 4.4, we will specify the corresponding restrictions and assumptions to obtain the classical 5-parameter shell formulation predominantly used for standard shell problems in the context of finite element analysis.

In most part of the text, we restrict ourselves to static problems within the framework of geometrically nonlinear elasticity, neglecting time dependence and inertia effects. The extension into the materially nonlinear area is a straightforward procedure. It is believed that this does not mean a too strong restriction in view of the underlying motivation.

It is a well cultivated tradition to let review articles start with the remark that a complete overview of existing methods and appropriate literature is utterly impossible. The multitude of existing concepts, methods, and implementations, as well as scientific papers, text books, and yet other review articles would effectively prohibit an exhaustive overview. J. E. Marsden and T. J. R. Hughes remark in what they call the ‘disclaimer’ of their famous book on *Mathematical Foundations of Elasticity* (Marsden and Hughes, 1983) that

‘This book is neither complete nor unbiased. Furthermore, we have not mentioned many deep and highly erudite works, nor have we elucidated alternative approaches to the subject. Any historical comments we make on subjects prior to 1960 are probably wrong, and credits to some theorems may be incorrectly assigned.’

Although the present paper is neither a book nor covers such a broad field like the textbook by Marsden and Hughes (1983), it clearly shares the quoted property. We therefore directly head toward the ideas and inspirations driving the authors during the compilation of the paper at hand.

Motivations for concerning oneself with the present subject are many. They might be of purely scientific nature or driven by the need to find the necessary level for the mechanical content of a model or to have a reliable element as a tool for certain applications one might have in mind. Interest in the mathematical formulation and resulting

numerical properties of finite elements for thin-walled structures may also arise when simply applying certain finite element formulations available in scientific or commercial codes. While trying to provide useful information for practitioners and users of commercial finite element codes, this treatise clearly addresses a readership with a scientific background, both things not being mutually exclusive anyway.

When developing and applying a finite element formulation for thin-walled structures, one comes across a couple of questions. Which mechanical effects should be included and which can be neglected? Is it better to start from a *shell theory* or develop *continuum-based* elements along the lines of the *degenerated solid* approach? And what about *geometrically exact* models? Which simplifications are useful – and admissible? Which consequences does the formulation have for the finite element model? Which parameterization of degrees of freedom are sensible for the applications one has in mind? Should drilling degrees of freedom be included in a shell formulation or not? There are many, many more questions.

It is in this spirit that we try to give an overview of the various decisions that one *implicitly* makes when choosing a specific *theory* or *finite element formulation*, respectively. Although such an overview is necessarily incomplete, it should not cover only a mere register of umpteen different plate and shell finite elements along with their alleged pros, cons, and limitations; to be even more specific, this aspect will be very limited in the present contribution.

By doing this, we carefully separate *model decisions* and the *finite element formulation*. The former addresses those approximations that are made while formulating the continuous theory. The latter is concerned with additional approximation errors, coming into play along with discretization and finite element formulation. While these numerical errors eventually vanish with mesh refinement, the model errors, inherent to the theory, persist. Distinguishing this is crucial for a sophisticated determination of feasible methods and a competent interpretation of numerical results.

1.3 Notation and conventions

Throughout this text, we are using both index notation and absolute notation for the expressions of vectors and tensors, trying to comply with standard conventions in modern papers and text books. In general, operators are printed as standard characters, scalars as italics, vectors and tensors are printed bold face italic. Quantities needed in both the undeformed (reference) and deformed (current) configurations are identified with uppercase and lowercase letters, respectively.

In order to avoid misunderstanding and confusion, some points that might need clarification are listed below. Let \mathbf{a} and \mathbf{b} be vectors, then

$$\mathbf{a} \cdot \mathbf{b} = \mathbf{a}^T \cdot \mathbf{b} = a_i b^i = a^i b_i \quad (1)$$

all expressions representing their inner product. The transpose, in a sense necessary in matrix notation, is usually omitted. For the scalar product of second-order tensors, we use the following notation:

$$\mathbf{A} : \mathbf{B} := A^{ij} \mathbf{g}_i \otimes \mathbf{g}_j : B_{kl} \mathbf{g}^k \otimes \mathbf{g}^l = A^{ij} B_{kl} \quad (2)$$

The tensor product (or dyadic product) of two vectors $\mathbf{a}, \mathbf{b} \in \mathbb{R}^3$ is implicitly defined by the relation

$$(\mathbf{a} \otimes \mathbf{b}) \cdot \mathbf{c} = \mathbf{a} \cdot (\mathbf{b} \cdot \mathbf{c}) \quad \forall \mathbf{c} \in \mathbb{R}^3 \quad (3)$$

When using index notation, like in Equation (1), Latin indices take values $\{1, 2, 3\}$ and Greek indices are restricted to $\{1, 2\}$. Superscripts mark contravariant components and subscripts indicate covariant components of vectors or tensors. Moreover, Einstein's summation convention

$$a_i b^i := \sum_{i=1}^3 a_i b^i \quad (4)$$

applies for both Latin and Greek indices if appearing twice within a product, like in Equation (1).

The norm (length) of a vector is defined as

$$\|\mathbf{a}\| := \sqrt{\mathbf{a} \cdot \mathbf{a}} = \sqrt{a^i a_i} \quad (5)$$

whereas the notation

$$|a| := \text{sgn}(a) a \quad (6)$$

defines the absolute value of a scalar quantity. Cartesian base vectors, their components referring to the global Cartesian frame, are given as

$$\begin{aligned} \mathbf{e}_1 = \mathbf{e}^1 &= \begin{bmatrix} 1 \\ 0 \\ 0 \end{bmatrix}, & \mathbf{e}_2 = \mathbf{e}^2 &= \begin{bmatrix} 0 \\ 1 \\ 0 \end{bmatrix}, \\ \mathbf{e}_3 = \mathbf{e}^3 &= \begin{bmatrix} 0 \\ 0 \\ 1 \end{bmatrix} \end{aligned} \quad (7)$$

Unless otherwise stated, vector and matrix coefficients arranged in between brackets always refer to a Cartesian frame. It is without loss of generality that a corresponding

embedding three-dimensional space is available. A subscripted (or superscripted) scalar put in between braces indicates a matrix

$$\{A_{ij}\} := \begin{bmatrix} A_{11} & A_{12} & A_{13} \\ A_{21} & A_{22} & A_{23} \\ A_{31} & A_{32} & A_{33} \end{bmatrix} \quad (8)$$

The gradient operator referring to the reference configuration is defined as

$$\begin{aligned} \text{Grad}(\mathbf{u}) &:= \frac{\partial \mathbf{u}}{\partial \mathbf{X}} = \frac{\partial \mathbf{u}}{\partial X^i} \otimes \mathbf{e}^i \\ &= \frac{\partial u_j}{\partial X^i} \mathbf{e}^j \otimes \mathbf{e}^i = \begin{bmatrix} \frac{\partial u_1}{\partial X^1} & \frac{\partial u_1}{\partial X^2} & \frac{\partial u_1}{\partial X^3} \\ \frac{\partial u_2}{\partial X^1} & \frac{\partial u_2}{\partial X^2} & \frac{\partial u_2}{\partial X^3} \\ \frac{\partial u_3}{\partial X^1} & \frac{\partial u_3}{\partial X^2} & \frac{\partial u_3}{\partial X^3} \end{bmatrix} \end{aligned} \quad (9)$$

The capital G in 'Grad' indicates that this operation refers to the reference configuration. X^i are the Cartesian coordinates of a material point in this configuration. Using curvilinear coordinates θ^i we can write

$$\begin{aligned} \text{Grad}(\mathbf{u}) &= \frac{\partial \mathbf{u}}{\partial X^i} \otimes \mathbf{e}^i = \frac{\partial \mathbf{u}}{\partial \theta^k} \frac{\partial \theta^k}{\partial X^i} \otimes \mathbf{e}^i \\ &= \frac{\partial \mathbf{u}}{\partial \theta^k} \otimes \frac{\partial \theta^k}{\partial X^i} \mathbf{e}^i = \frac{\partial \mathbf{u}}{\partial \theta^k} \otimes \frac{\partial \theta^k}{\partial \mathbf{X}} = \mathbf{u}_{,k} \otimes \mathbf{G}^k \end{aligned} \quad (10)$$

Abbreviation of partial derivatives with a subscripted comma

$$a_{,i} := \frac{\partial a}{\partial \theta^i} \quad (11)$$

always refer to curvilinear coordinates, as indicated. The divergence of a tensor field is given by

$$\text{Div}(\mathbf{A}) := \frac{\partial \mathbf{A}}{\partial X^k} \cdot \mathbf{e}^k = \frac{\partial A_{ij}}{\partial X^k} (\mathbf{e}^i \otimes \mathbf{e}^j) \cdot \mathbf{e}^k = \begin{bmatrix} \frac{\partial A_{1i}}{\partial X^i} \\ \frac{\partial A_{2i}}{\partial X^i} \\ \frac{\partial A_{3i}}{\partial X^i} \end{bmatrix} \quad (12)$$

which, in curvilinear coordinates, reads

$$\begin{aligned} \text{Div}(\mathbf{A}) &= \frac{\partial \mathbf{A}}{\partial \theta^k} \cdot \mathbf{g}^k = (A_{,k}^{ij} \mathbf{g}_i \otimes \mathbf{g}_j) \cdot \mathbf{g}^k \\ &\quad + (A^{ij} \mathbf{g}_{i,k} \otimes \mathbf{g}_j) \cdot \mathbf{g}^k + (A^{ij} \mathbf{g}_i \otimes \mathbf{g}_{j,k}) \cdot \mathbf{g}^k \\ &= A_{,j}^{ij} \mathbf{g}_i + A^{ij} \mathbf{g}_{i,j} + A^{ij} \mathbf{g}_i \cdot (\mathbf{g}_{j,k} \cdot \mathbf{g}^k) \end{aligned} \quad (13)$$

Finally, the determinant $\text{Det}(\mathbf{A})$ of a second-order tensor \mathbf{A} is defined as a measure for the change of volume of

a parallelepiped formed by three arbitrary vectors \mathbf{a} , \mathbf{b} , \mathbf{c} when transformed by \mathbf{A} ,

$$\text{Det}(\mathbf{A}) := \frac{(\mathbf{A} \cdot \mathbf{a}) \cdot ((\mathbf{A} \cdot \mathbf{b}) \times (\mathbf{A} \cdot \mathbf{c}))}{\mathbf{a} \cdot (\mathbf{b} \times \mathbf{c})} \quad (14)$$

The definition is independent of the choice of \mathbf{a} , \mathbf{b} , and \mathbf{c} and the determinant is invariant under a change of basis. Utilizing Cartesian base vectors recovers the well-known formula for computation of determinants of square matrices.

2 MATHEMATICAL AND MECHANICAL FOUNDATIONS

2.1 Differential geometry of surfaces and bodies in space

In the description of differential geometry and kinematics, the language of classical tensor analysis is used, although a large number of recent treatises on continuum mechanics unfold upon the theory of differentiable manifolds; see, for instance, Simo and Hughes (1998); Marsden and Hughes (1983). The latter concept is more general and particularly useful in cases where embedding spaces of higher order are not available. This is the case, for instance, in the context of the theory of relativity, which has at the same time been one of the major motivations for the further development of differential geometry of manifolds.

However, as long as we are dealing with processes taking place in \mathbb{R}^3 , with space and time being decoupled, there does not seem to be a need to plunge into the advanced mathematical framework of differential geometry of manifolds, other than elegance or generality. Therefore, in the spirit of an Encyclopedia, we tried to put together concepts and formulae that are directly accessible to comparison and implementation, at the same time trying to keep compromises with respect to mathematical rigor within bearable limits.

The position vector of a given point on a *surface* in three-dimensional space is denoted by $\mathbf{R}(\theta^1, \theta^2)$, where convective coordinates θ^α ought to represent a singularity-free parameterization, that is, θ^1 and θ^2 uniquely identify a specific location on the surface and each location on the surface is uniquely associated with a pair of coordinates $\{\theta^1, \theta^2\}$ (Figure 1). We will later on additionally introduce the θ^3 -direction, indicating the thickness direction needed to associate the surface with a three-dimensional body.

Likewise, a position vector to a point in a *three-dimensional body* is denoted as $\mathbf{X}(\theta^1, \theta^2, \theta^3)$. We will presume in the following that the body under consideration

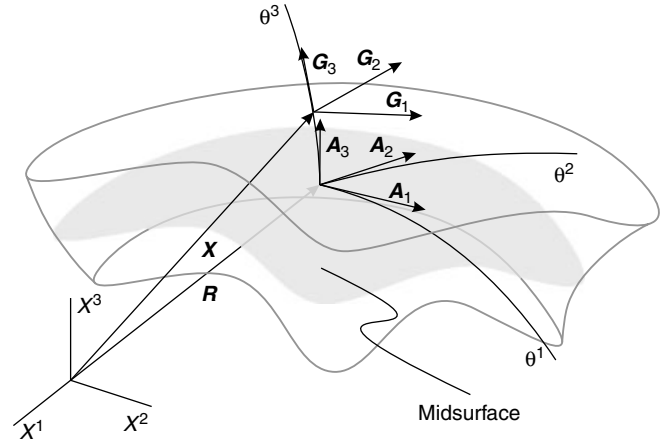


Figure 1. Geometry of shell-like body. A color version of this image is available at <http://www.mrw.interscience.wiley.com/ecom>

contains the aforementioned surface – its *midsurface* – as a subset such that

$$\begin{aligned} \mathbf{X}(\theta^1, \theta^2, 0) &= \mathbf{X} |_{\theta^3=0} = \mathbf{R}(\theta^1, \theta^2), \\ \theta^3 &\in \left[-\frac{t(\theta^1, \theta^2)}{2}, \frac{t(\theta^1, \theta^2)}{2} \right] \end{aligned} \quad (15)$$

with $t(\theta^1, \theta^2)$ being the shell thickness. Covariant base vectors are obtained from partial derivatives of the corresponding position vectors with respect to the convective coordinates in either case, namely,

$$\mathbf{G}_i = \mathbf{X}_{,i} \quad \mathbf{A}_i = \mathbf{G}_i |_{\theta^3=0} \quad (16)$$

As \mathbf{R} is a function of θ^1 and θ^2 , only two covariant base vectors on the midsurface $\mathbf{A}_\alpha = \mathbf{R}_{,\alpha}$ can be computed directly. Therefore, if a three-dimensional tangent space to a two-dimensional surface is needed, \mathbf{A}_3 has to be constructed somehow. One self-suggesting possibility is to define

$$\mathbf{A}_3 := \frac{\mathbf{A}_1 \times \mathbf{A}_2}{\|\mathbf{A}_1 \times \mathbf{A}_2\|} =: \mathbf{D} \quad (17)$$

In the context of shell theories, the normalized normal vector \mathbf{D} , defined in Equation (17) is called the *director*.

Metric tensors on the surface, and within the body, respectively, are given by

$$\mathbf{A} = A_{ij} \mathbf{A}^i \otimes \mathbf{A}^j \quad (18)$$

$$\mathbf{G} = G_{ij} \mathbf{G}^i \otimes \mathbf{G}^j \quad (19)$$

where

$$A_{ij} = \mathbf{A}_i \cdot \mathbf{A}_j, \quad G_{ij} = \mathbf{G}_i \cdot \mathbf{G}_j \quad (20)$$

For the sake of completeness, we define the *second fundamental form*

$$B_{\alpha\beta} := \frac{1}{2}(A_{\alpha} \cdot A_{3,\beta} + A_{\beta} \cdot A_{3,\alpha}) \quad (21)$$

and *Gaussian curvature*

$$K = \frac{\text{Det}\{-B_{\alpha\beta}\}}{\text{Det}\{A_{\alpha\beta}\}} \quad (22)$$

Finally, the *mean curvature* is defined as

$$H = \frac{1 - B_{11}A_{22} + 2B_{12}A_{12} - B_{22}A_{11}}{2 \text{Det} A_{\alpha\beta}} \quad (23)$$

and principal curvatures R_{α} are given implicitly by

$$\begin{aligned} \frac{1}{R^2} - 2H\frac{1}{R} + K &= 0 \\ \Rightarrow \begin{cases} R_{1,2} = \frac{H \pm \sqrt{H^2 - K}}{K} & \text{for } K > 0 \\ R_1 = \frac{1}{2H}, \quad R_2 = \infty & \text{for } K = 0 \end{cases} \end{aligned} \quad (24)$$

2.2 Continuum mechanics

The mathematical theory of nonlinear continuum mechanics is treated in numerous papers and text books and there is neither space nor need at this point to review it in detail. The intention of this section is to introduce the notation used in the subsequent sections and to provide some of the basic formulae needed for the derivations therein. At the same time, we narrow down the vast field of nonlinear continuum mechanics to the type of problems that we utilize in the sequel to develop plate and shell models in view of their respective finite element discretizations. The mechanical derivations in this section are concluded when arriving at the field equations and boundary conditions that specify the boundary value problem of three-dimensional, nonlinear elasticity.

As the equilibrium equations and the force boundary conditions are usually represented in the weak form in the context of finite element methods, a brief description of the underlying variational formulation concludes this section.

Although some remarks on nonlinear dynamics are scattered throughout the text, most of the mathematical derivations are restricted to time-independent problems, neglecting inertia effects. We will therefore refrain from discussing topics like Hamiltonian mechanics. The scalar variable t will be used as a pseudo-time in order to be able to parameterize sequences of configurations (i.e. quasi-static deformations). Confusion with plate or shell thickness, for

which the same variable is used, should be excluded in the respective context.

For further studies in nonlinear continuum mechanics, we recommend (in alphabetical order) the treatises by Duvaut and Lions (1972), Green and Zerna (1968), Gurtin (1981), Malvern (1969), Marsden and Hughes (1983), Stein and Barthold (1996), Sokolnikoff (1956) as well as Truesdell and Noll (1965).

Point of departure is the introduction of a set \mathfrak{B} of connected material points \mathfrak{M}_i , which we identify with a *body*. The surface, or *boundary* of the body is denoted as $\partial\mathfrak{B}$. Unless otherwise specified, all equations given in this section are assumed to be valid in the domain \mathfrak{B} . The placement of \mathfrak{B} , that is, of its individual material points in space, is called *configuration* and can formally be defined as

$$\chi: (\mathfrak{B}, t) \rightarrow \mathfrak{S} \quad (25)$$

The map χ associates a unique *position vector* $\mathbf{x} \in \mathbb{R}^3$ in three-dimensional space with each material point $\mathfrak{M}_i \in \mathfrak{B}$ and time $t \in [t_0, \infty]$.

Equation (25) effectively introduces the notion of non-polar polar continuum mechanics. This means that the configuration at a certain time t is uniquely defined by a set of position vectors $\mathbf{x} \in \mathbb{R}^3$. *Polar* continuum mechanical concepts, usually associated with the names of the Cosserats (Cosserat and Cosserat, 1909), require additional information about the orientation of the material points, or so-called directors associated with those. This concept will be of some significance in the context of geometrically exact shell formulations, introduced in Section 4.2.

The configuration at $t = t_0$ is called *reference configuration*, and it is usually understood to be the undeformed state of the structure. As said already, following a standard convention in continuum mechanics, we mark quantities referring to the reference configuration with uppercase letters, such that, for instance, \mathbf{X} denotes the position vector to a material point in its placement at time $t = t_0$. The components X^i of $\mathbf{X} = X^i \mathbf{e}_i$ are therefore also called *material coordinates* of the body.

The *current configuration* of the body at a given time $t > t_0$ can now be formulated as a map from the reference configuration onto \mathbb{R}^3 ,

$$\Phi: (\mathbf{X}, t) \rightarrow \mathbb{R}^3 \quad (26)$$

In this sense, a *deformation process* can be understood as a continuous sequence of configurations $\Phi(\mathbf{X}, t)$. (Strictly speaking, interpretation as a deformation *process* is not quite correct as we already explicitly excluded time dependency. This somewhat captious distinction of a continuous

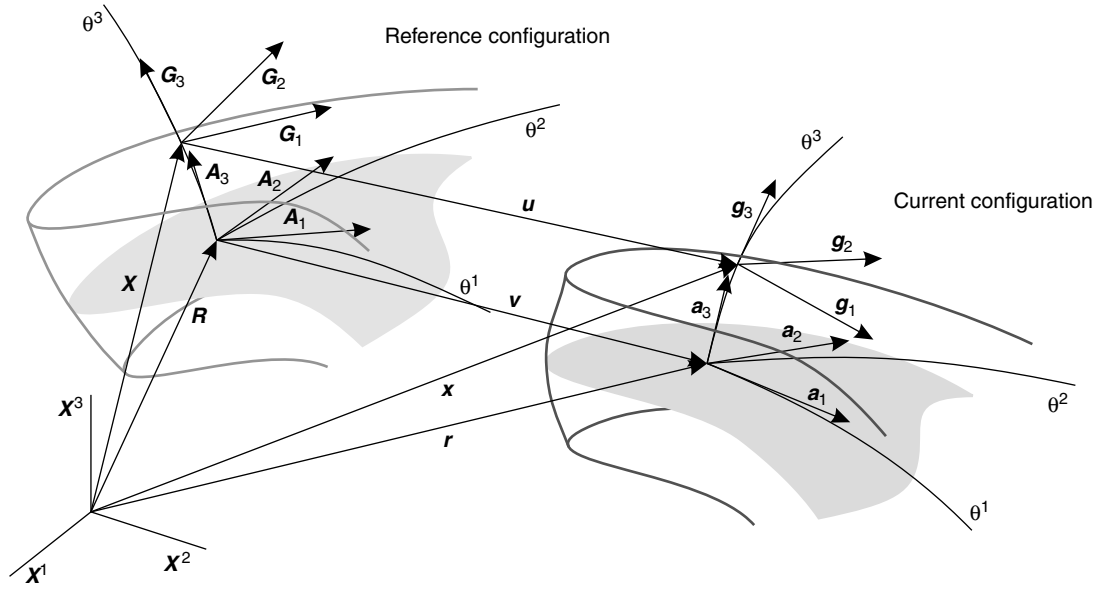


Figure 2. Deformation, reference and current configuration. A color version of this image is available at <http://www.mrw.interscience.wiley.com/ecm>

set of states of deformation and an actual deformation process may be of some importance in the context of stability problems).

Quantities referring to the current (or deformed) configuration are written as lowercase letters. For the position vector of a material point \mathfrak{M}_i identified by its position vector \mathbf{X} at time $t = t_0$ we therefore write

$$\mathbf{x} = \Phi(\mathbf{X}, t) \quad (27)$$

In the following, we will frequently directly understand the position vector itself as being a function of the material coordinates and time, $\mathbf{x} = \mathbf{x}(\mathbf{X}, t)$. Although mathematically this is a bit sloppy, it does not affect the validity of the resulting equations from a practical, that is, implementation-oriented point of view. Likewise, we are using Ω and Γ , respectively, for the denomination of the domain of the problem, that is, the body \mathfrak{B} and its boundary $\partial\mathfrak{B}$, respectively, because this notation complies with what one commonly finds in finite element related literature.

As illustrated in Figure 2, the *displacements* are defined as the difference between position vectors in the current and the reference configuration, respectively,

$$\mathbf{u}(\mathbf{X}, t) = \mathbf{x}(\mathbf{X}, t) - \mathbf{X} \quad (28)$$

For the description of the actual deformation of the body, information about the shape of infinitesimal volume elements is needed. Mathematically, this information is represented by the three-dimensional tangent spaces to the corresponding material points. The covariant base vectors,

associated with those spaces, are given by equation (16) in the reference configuration and by

$$\mathbf{g}_i = \mathbf{x}_{,i} \quad (29)$$

in the current configuration. The partial derivatives are taken with respect to the convective, curvilinear coordinates θ^i .

It is convenient to define the contravariant base vectors $\mathbf{G}^i = (\partial\theta^i/\partial\mathbf{X})$ via the orthogonality condition $\mathbf{G}^i \cdot \mathbf{G}_j = \delta_j^i$. It leads to

$$\mathbf{G}^i = G^{ij} \mathbf{G}_j, \quad \text{with } \{G^{ij}\} = \{G_{ij}\}^{-1} \quad (30)$$

Similar definitions apply to the current configuration. The relationship between covariant base vectors of both configurations is accomplished by applying the chain rule

$$\mathbf{g}_i = \frac{d\mathbf{x}}{d\theta^i} = \frac{d\mathbf{x}}{d\mathbf{X}} \cdot \frac{d\mathbf{X}}{d\theta^i} = \mathbf{F} \cdot \mathbf{G}_i \quad (31)$$

where

$$\begin{aligned} \mathbf{F} = \text{Grad } \mathbf{x} &= \frac{d\mathbf{x}}{d\mathbf{X}} = \frac{\partial \mathbf{x}}{\partial X^i} \otimes \mathbf{e}^i = \frac{\partial \mathbf{x}}{\partial \theta^k} \frac{\partial \theta^k}{\partial X^i} \otimes \mathbf{e}^i \\ &= \frac{\partial \mathbf{x}}{\partial \theta^k} \otimes \frac{\partial \theta^k}{\partial X^i} \mathbf{e}^i = \frac{\partial \mathbf{x}}{\partial \theta^k} \otimes \frac{\partial \theta^k}{\partial \mathbf{X}} = \mathbf{g}_k \otimes \mathbf{G}^k \end{aligned} \quad (32)$$

is called the *material deformation gradient*. Covariant and contravariant base vectors of both configurations can be

transferred with the help of the following formulae:

$$\begin{aligned} \mathbf{g}_i &= \mathbf{F} \cdot \mathbf{G}_i, & \mathbf{g}^i &= \mathbf{F}^{-T} \cdot \mathbf{G}^i, & \mathbf{G}_i &= \mathbf{F}^{-1} \cdot \mathbf{g}_i, \\ \mathbf{G}^i &= \mathbf{F}^T \cdot \mathbf{g}^i \end{aligned} \quad (33)$$

The first two procedures, mapping quantities from the reference to the current configuration, are called *push forward* operations, the other ones are denoted as *pull back*.

Solving equations (33) for \mathbf{F} provides a couple of useful formulae for computation of the deformation gradient and its inverse:

$$\begin{aligned} \mathbf{F} &= \mathbf{g}_i \otimes \mathbf{G}^i, & \mathbf{F}^{-T} &= \mathbf{g}^i \otimes \mathbf{G}_i, & \mathbf{F}^{-1} &= \mathbf{G}_i \otimes \mathbf{g}^i, \\ \mathbf{F}^T &= \mathbf{G}^i \otimes \mathbf{g}_i \end{aligned} \quad (34)$$

The deformation gradient \mathbf{F} is a generally nonsymmetric second-order tensor. In order to uniquely accomplish the transformations in equations (31) it has to be invertible. This requires its determinant, the *Jacobian* $J = \text{Det}(\mathbf{F})$ to be nonzero. Moreover, the map associated with \mathbf{F} ought to be continuous and hence we arrive at the requirement of positive semidefiniteness

$$J = \text{Det}(\mathbf{F}) \geq 0 \quad (35)$$

Mechanically, this condition precludes self-penetration of material.

From the numerous *strain measures*, suitable also for the description of problems involving large strains, we will use the *Green–Lagrangean* strain tensor

$$\mathbf{E} = \frac{1}{2}(\mathbf{F}^T \cdot \mathbf{F} - \mathbf{G}) \quad (36)$$

in the following (note that \mathbf{G} represents the identity tensor in equation (36)). Alternative representations of \mathbf{E} , referring to covariant components with respect to the metric of the reference configuration, are

$$\begin{aligned} \mathbf{E} &= E_{ij} \mathbf{G}^i \otimes \mathbf{G}^j, & E_{ij} &= \frac{1}{2}(\mathbf{u}_{,i} \cdot \mathbf{G}_j + \mathbf{u}_{,j} \cdot \mathbf{G}_i + \mathbf{u}_{,i} \cdot \mathbf{u}_{,j}) \\ &= \frac{1}{2}(g_{ij} - G_{ij}) \end{aligned} \quad (37)$$

where $g_{ij} = \mathbf{g}_i \cdot \mathbf{g}_j$ (cf. equation (20)).

In most parts of this paper, we will refer to geometrically nonlinear formulations, using the Green–Lagrangean strain tensor given in equations (36) and (37). However, in the context of plates, we will also refer to its linearized version, given here without reproducing detailed derivations as

$$\begin{aligned} \mathbf{E}^L &= E_{ij}^L \mathbf{G}^i \otimes \mathbf{G}^j, & E_{ij}^L &= \frac{1}{2}(\mathbf{u}_{,i} \cdot \mathbf{G}_j + \mathbf{u}_{,j} \cdot \mathbf{G}_i) \\ &= \frac{1}{2}(\mathbf{g}_i \cdot \mathbf{G}_j + \mathbf{g}_j \cdot \mathbf{G}_i - 2G_{ij}) \end{aligned} \quad (38)$$

The energetically conjugate quantity to \mathbf{E} is the *second Piola–Kirchhoff stress tensor* \mathbf{S} . As the latter refers to the undeformed configuration, although its components follow the deforming line elements, it is not directly accessible to physical interpretation. The *Cauchy stress tensor* $\boldsymbol{\sigma}$, whose components refer to the current configuration and thus represent the actual physical straining of the material, is obtained from \mathbf{S} via

$$\boldsymbol{\sigma} = J^{-1} \mathbf{F} \cdot \mathbf{S} \cdot \mathbf{F}^T \quad (39)$$

Equation (39) will be important later on when defining mechanically meaningful stress resultants.

In order to keep the derivations in the subsequent chapters as simple as possible, we refer to a linear *St. Venant–Kirchhoff*-type material law. Its application is sensible for material and structural behavior exhibiting small strains but large rotations. The framework developed so far, however, is also directly accessible to materials leading to large strains like in hyper-elasticity or finite strain elastoplasticity (see, for instance, the text books by Belytschko, Liu and Moran (2000) and Simo and Hughes (1998)); the same is true for formulations for thin-walled structures that follow.

Assuming the existence of an elastic potential, the fourth-order *material tensor* (sometimes also called *elasticity tensor*) is given by

$$\mathbf{C} = \frac{\partial^2 W^{\text{int}}(\mathbf{E})}{\partial \mathbf{E} \partial \mathbf{E}} \quad (40)$$

with the *strain energy density* $W^{\text{int}}(\mathbf{E})$. For a St. Venant–Kirchhoff-type material law, \mathbf{C} establishes a unique linear relationship between \mathbf{E} and \mathbf{S} via

$$\mathbf{S} = \mathbf{C} : \mathbf{E} \quad (41)$$

In order to make the scalar product of strains and stresses, representing the internal work, independent of the coordinate system, contravariant components are usually preferred for the representation of \mathbf{S} . Thus,

$$\begin{aligned} \mathbf{S} &= S^{ij} \mathbf{G}_i \otimes \mathbf{G}_j \rightarrow \mathbf{E} : \mathbf{S} = E_{ij} S^{kl} (\mathbf{G}^i \otimes \mathbf{G}^j) : (\mathbf{G}_k \otimes \mathbf{G}_l) \\ &= E_{ij} S^{kl} \delta_k^i \delta_l^j = E_{ij} S^{ij} \end{aligned} \quad (42)$$

The fourth-order tensor \mathbf{C} has $3^4 = 81$ components C^{ijkl} in the first place. As strains and stresses are symmetric in our context, the number of *independent* components reduces to $6 \cdot 6 = 36$. The corresponding symmetries $C_{ijkl} = C_{jilk}$ are sometimes referred to as *minor symmetries* in the literature. Moreover – given sufficient smoothness of the potential

W^{int} – we have

$$C_{ijkl} = \frac{\partial^2 W^{\text{int}}}{\partial E_{ij} \partial E_{kl}} = \frac{\partial^2 W^{\text{int}}}{\partial E_{kl} \partial E_{ij}} = C_{klij} \quad (43)$$

further reducing the number of independent constants to 21. The corresponding symmetries $C_{ijkl} = C_{klij}$ are called *major symmetries*. Representation of the resulting material matrix in Voigt notation can thus be given as

$$\{C_{(ij)(kl)}\} = \begin{bmatrix} C_{1111} & C_{1122} & C_{1133} & C_{1123} & C_{1113} & C_{1112} \\ & C_{2222} & C_{2233} & C_{2223} & C_{2213} & C_{2212} \\ & & C_{3333} & C_{3323} & C_{3313} & C_{3312} \\ & & & C_{2323} & C_{2313} & C_{2312} \\ & \text{symm.} & & & C_{1313} & C_{1312} \\ & & & & & C_{1212} \end{bmatrix} \quad (44)$$

The reader is referred to Belytschko, Liu and Moran (2000) and references therein for a definition of Voigt notation and further reading. For a discussion of the topic of material symmetries see, for instance, Nye (1985). In the appendix, equation (44) is substantiated for the important case of orthotropic material.

For the case of material isotropy, two independent parameters are sufficient to completely characterize linear material behavior. In engineering literature, usually *Young's modulus* E and *Poisson's ratio* ν are preferred. In mathematical texts, one frequently finds the so-called *Lamé constants*

$$\lambda = \frac{\nu E}{(1 + \nu)(1 - 2\nu)} \quad \text{and} \quad \mu = \frac{E}{2(1 + \nu)} \quad (45)$$

The curvilinear components of the elasticity tensor are then given by

$$C^{ijkl} = \lambda G^{ij} G^{kl} + \mu (G^{ik} G^{jl} + G^{il} G^{jk}),$$

$$\mathbf{C} = C^{ijkl} \mathbf{G}_i \otimes \mathbf{G}_j \otimes \mathbf{G}_k \otimes \mathbf{G}_l \quad (46)$$

and

$$S^{ij} = C^{ijkl} E_{kl} \quad (47)$$

Equations (36) and (47) represent two of three governing field equations of the aforementioned boundary-value problem. The lacking *balance of linear momentum* (or *equilibrium condition*) reads

$$\text{Div}(\mathbf{F} \cdot \mathbf{S}) + \rho \mathbf{b} = \mathbf{0} \quad (48)$$

As already mentioned, in view of a finite element discretization we will focus on the weak form of equilibrium.

Appropriate boundary conditions are given by

$$\mathbf{u} = \hat{\mathbf{u}} \quad \text{on } \Gamma_u \quad (49)$$

for the displacements and

$$\mathbf{F} \cdot \mathbf{S} \cdot \mathbf{n} = \hat{\mathbf{t}} \quad \text{on } \Gamma_\sigma \quad (50)$$

for the surface traction. Here, $\hat{\mathbf{u}}$ denotes prescribed displacements on the corresponding part Γ_u of the boundary and $\hat{\mathbf{t}}$ are prescribed surface tractions on Γ_σ .

For a displacement formulation, equation (49) describes *Dirichlet* boundary conditions, whereas equation (50) are the *Neumann* boundary conditions. Mixed, so-called *Robin* boundary conditions – appearing for instance in the case of elastic support – are not further discussed.

The variational basis for finite element formulations in structural mechanics are usually energy functionals. For the simplest and most popular type, namely, the aforementioned displacement-based finite elements relying on a standard Galerkin formulation with the displacement field as the only primary unknown, this is the *virtual work principle* (sometimes also called *principle of virtual displacements*),

$$\delta \Pi = \int_{\Omega} [\mathbf{S} : \delta \mathbf{E} - \rho \mathbf{b} \cdot \delta \mathbf{u}] d\Omega - \int_{\Gamma_\sigma} \hat{\mathbf{t}} \cdot \delta \mathbf{u} d\Gamma = 0 \quad (51)$$

Mathematically, equation (51) is the weak form of equilibrium, equation (48), and force boundary conditions, equation (50). It is subject to two local subsidiary conditions

$$\mathbf{E} = \frac{1}{2}(\mathbf{F}^T \cdot \mathbf{F} - \mathbf{G}) \quad \text{and} \quad \mathbf{S} = \mathbf{S}(\mathbf{E}) \quad (52)$$

representing the kinematic equation and the material law, and one subsidiary condition on the boundary, namely, the displacement boundary condition, equation (49). The variation of \mathbf{E} can be expressed as

$$\delta \mathbf{E} = \frac{1}{2}(\delta \mathbf{F}^T \cdot \mathbf{F} + \mathbf{F}^T \cdot \delta \mathbf{F})$$

$$= \frac{1}{2}(\delta \mathbf{u}_{,X}^T \cdot \mathbf{G} + \delta \mathbf{u}_{,X}^T \cdot \mathbf{u}_{,X} + \mathbf{G}^T \cdot \delta \mathbf{u}_{,X} + \mathbf{u}_{,X}^T \cdot \delta \mathbf{u}_{,X}) \quad (53)$$

The virtual work principle states that the work done by the external forces $\rho \mathbf{b}$ (body forces) and $\hat{\mathbf{t}}$ (surface tractions) in an arbitrary virtual displacement $\delta \mathbf{u}$ (also called *test function*) is zero if the mechanical system is in a state of static equilibrium. The virtual displacements have to comply with kinematic constraints, that is, they have to be admissible, exactly complying with the kinematic equations and displacement boundary conditions. The consequence for a finite element formulation is that shape functions used for discretization of virtual displacements (test functions) have to vanish on Γ_u and those used for displacements (trial

functions) have to comply with the displacement boundary conditions (49). Moreover, both test and trial functions ought to obey certain compatibility and completeness conditions in order to ensure consistence and thus convergence of the finite element method. These issues are discussed in detail in **Chapter 4 of Volume 1**.

In the context of functional analysis and variational calculus, the virtual displacements are called *variations*. In the case of conservative problems for which there exists a potential, equation (51) can be obtained from the *principle of minimum potential energy* with the standard methods of variational calculus. However, in a more general context, it can also be computed directly from the governing differential equations, namely, the equilibrium equation and the force boundary condition, with the help of the *method of weighted residuals* and integration by parts. Its validity does therefore not require existence of a potential. The corresponding finite elements can be applied directly to a wide range of nonlinear problems, not presupposing any external or internal potential.

When applying multifield variational principles, variations of strains and stresses may also appear. This applies, for instance, to the *Hellinger–Reissner* principle and the *Hu–Washizu* principle, prompting formulation of *mixed* or *hybrid-mixed* finite elements. In those elements, not only displacements but also stresses and/or strains appear as free variables.

For treatises on functional analysis and variational principles in mechanics, especially in the context of finite elements, we recommend (in alphabetical order) Bufler (1983), Felippa (1989, 1994), Oden and Reddy (1976), Reddy (1998) as well as Washizu (1968).

3 PLATES AND SHELLS

Shells are commonly identified as surface-like structures with one dimension being significantly smaller than the other two. Geometry of a – sufficiently smooth – shell can be uniquely identified by defining its midsurface and a thickness function. Shells play an important role in a lot of fields of nature and technology. They appear as containers, pipes, cooling towers, masonry cupolas, airplane fuselages, car bodies, egg shells, external skeletons of insects, and in an infinite number of other shapes. Plate and shell structures are often supplemented by slender stiffeners. They allow the thin-walled structure to keep their optimal load-carrying capacity without giving up their lightweight property. A thin structure with a heterogeneous layout across the thickness, for example, having a porous lightweight core, aims in the same direction.

If properly designed as load-carrying structures, shells exhibit an optimal ratio of stiffness to weight. In this case,

they carry the load exclusively via membrane forces, that is, forces parallel to the midsurface. In contrast to arches, in the case of doubly curved shells this can be achieved for more than just one specific load distribution. On the other hand, especially thin shells can be extremely sensitive to imperfections, specifically with regard to their stability behavior. This mixture of performance and sensitivity makes the shell the ‘primadonna of structures’ (Ramm, 1986). It is not at least for this reason that reliable methods for the analysis of shells are particularly important.

Structural behavior of shells is characterized by two principally different states of deformation, namely, *membrane* and *bending* action. Figure 3 shows some illustrative examples: the bending dominated deformations shown on the left-hand side exhibit typical ovalizing shapes, at least approximately preserving lengths of fibers in the midsurface. In contrast to that, membrane dominated deformations come along with strains in the midsurface, as shown on the right-hand side.

For designers, the membrane state is the desired one because it optimally makes use of the material, exhibiting an – at least approximately – constant stress distribution across the thickness. In the presence of bending, only the material fibers away from the midsurface are used and consequently, shells are much more flexible with respect to bending. Pure bending deformations of shells are also called *inextensional deformations* because there exists a surface within the shell that is completely free from longitudinal extension (or compression). Strictly speaking, pure inextensional deformations are only possible for developable structures (flat plates, cylinders, and cones). However, nearly inextensional deformations have a great practical significance also for doubly curved shells.

A particular stress situation can be classified as either *membrane dominated* or *bending dominated*, depending on the geometry of the shell, loads, and boundary conditions. Identification of one or the other situation can be

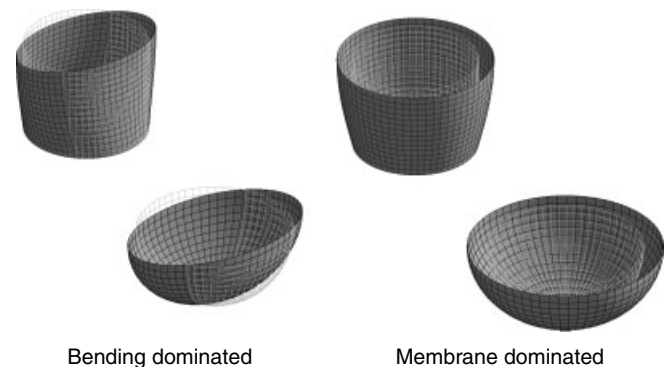


Figure 3. Typical examples for shells dominated by bending or membrane action. A color version of this image is available at <http://www.mrw.interscience.wiley.com/ecm>

accomplished on the basis of the *asymptotic behavior* of the shell as thickness approaches zero. The ratio of membrane energy to bending energy then either approaches infinity or zero, indicating a membrane dominated situation in the former case and a bending dominated one in the latter. Practical situations usually involve both membrane and bending action. However, for a well-designed load-carrying shell, structural behavior should be dominated by membrane action and bending may be present mainly due to unavoidable circumstances like concentrated forces or incompatibilities near boundaries. In the latter case, bending moments appear in the shape of boundary layers, the dimensions of which depend on shell thickness.

On the other hand, the feature of inextensible deformations may also be exploited in special cases. For example, deployable and inflatable structures should be designed to benefit from these bending dominated transition processes. Antennae unfolding in space, tape-like structures, for example, videotapes, and pneumatic structures under internal prestress are typical examples. They benefit from bending during the folding phase, eventually leading to a membrane dominated situation for their final application.

To illustrate some typical phenomena, we investigate the simple case of a clamped hemispherical shell subject to dead load in a numerical experiment. In Figure 4, the normalized energy fractions emanating from membrane forces and bending moments are plotted versus shell slenderness.

The shell essentially carries the load by membrane action but exhibits the typical boundary layer at the clamped edge. It results from the geometric constraint imposed by the boundary conditions, which is contradictory to a pure membrane state. The colored plots in Figure 4 show the distribution of the corresponding energy fractions. Clearly, the diminishing edge effect can be observed, reducing bending energy eventually to a tiny boundary layer effect. As a consequence, bending and membrane energy interchange their dominance from thick to thin.

The gradual transition from an initially bending dominated into a membrane dominated structure is also often the natural result of a nonlinear large deformation process during loading. A typical example is a well-supported flat plate being loaded perpendicular to its surface exploiting the membrane or hammock effect. In other words, the structure deforms into the optimal stress situation; it escapes from bending.

In mathematical literature, the terms *inhibited* and *non-inhibited* inextensional deformations are sometimes used, meaning that pure bending deformations are either excluded, for instance, by geometry or boundary conditions, or not excluded (Bathe and Chapelle, 2003). Those terms, however, are not equivalent to ‘membrane dominated’ and ‘bending dominated’.

Owing to the high flexibility of thin shells with respect to bending, this state of deformation has the strongest

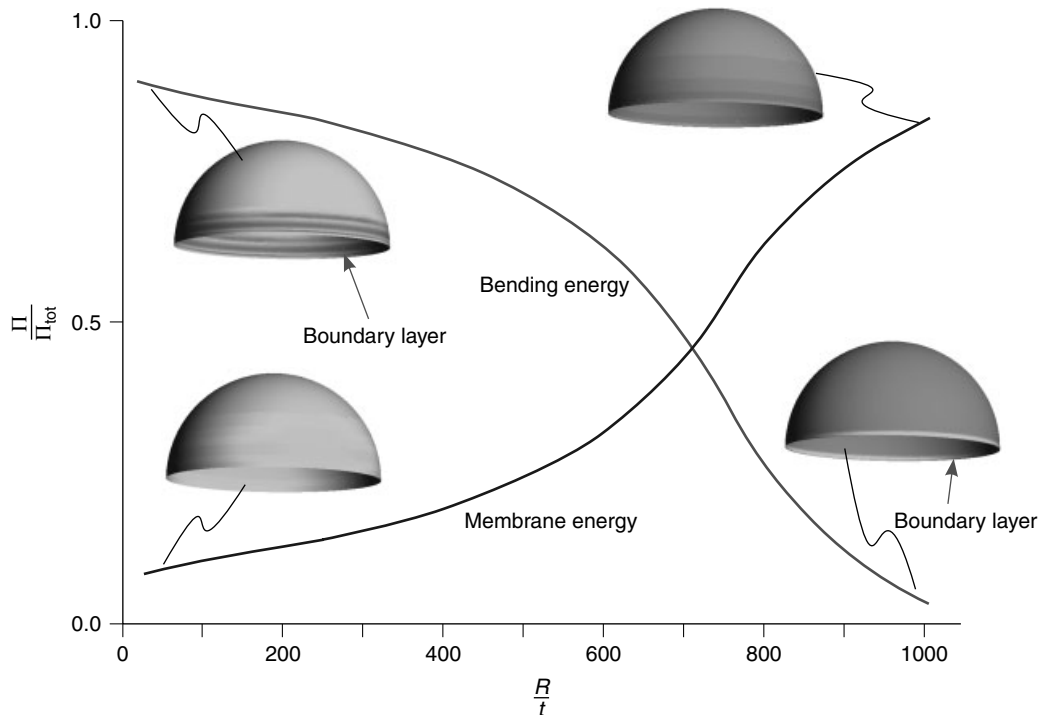


Figure 4. Evolution of strain energy fractions for a clamped hemispherical shell. A color version of this image is available at <http://www.mrw.interscience.wiley.com/ecm>

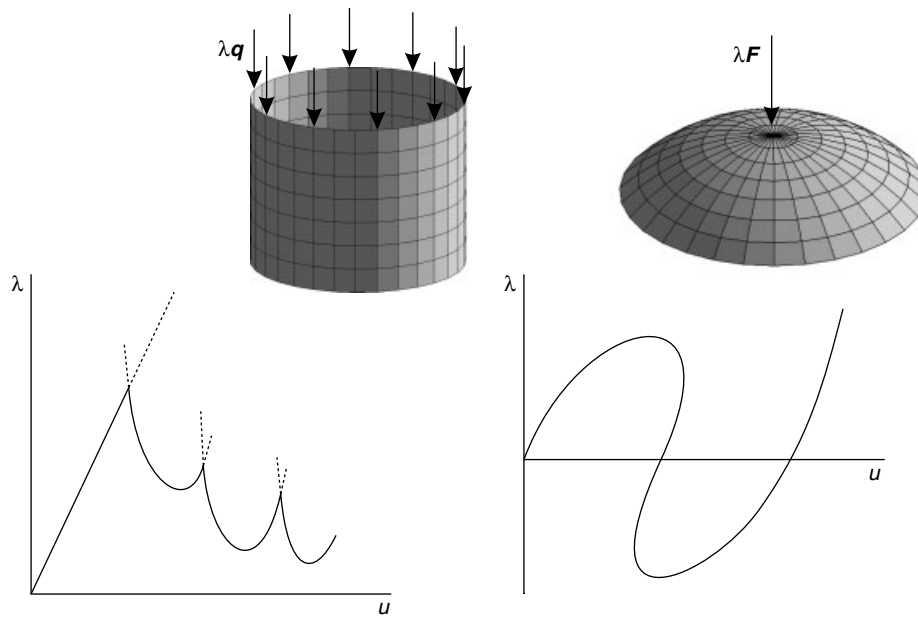


Figure 5. Nonlinear behavior of shells, buckling and snap-through. A color version of this image is available at <http://www.mrw.interscience.wiley.com/ecm>

impact on nonlinear behavior of shells. But also, shells in a pure membrane state may exhibit strong nonlinearities in the form of a sudden transition to a bending dominated state. This phenomenon, for example, through *buckling*, is typical for thin-walled structures and represents the reason for many spectacular accidents (Ramm and Wall, 2004), **Chapter 4 of this Volume**.

Figure 5 (left) shows a typical situation in which buckling may occur. A circular cylinder is subject to longitudinal load q . Observing the vertical displacement u while increasing the load parameter λ yields an almost perfectly linear behavior at first. As the critical load is reached, structural behavior instantly changes dramatically, the deformation changing from simple longitudinal compression to a typical buckling pattern, involving local bending effects. As can be seen from the load-displacement curve, this comes along with a sudden change in stiffness. The further development of structural behavior, exemplarily sketched in the diagram, exhibits additional bifurcation points at each of which the buckling patterns are changing – usually decreasing the number of buckles in circumferential direction while increasing the size of the individual buckles.

Another typical phenomenon involving strong nonlinearities is characterized by a gradual reduction of the *structural* stiffness (maybe even further triggered by reduction of the material stiffness), which eventually becomes negative. If the structural layout allows for very large deformations, the stiffness may become positive later on. A typical example is the snap-through of the spherical cap under a vertical load shown on the right-hand side of Figure 5.

In both cases, the parts of the load-displacement curves – more rigorously denoted as *static equilibrium paths* – that are descending to the right are unstable in the given configurations. In practical load-controlled experiments, the essentially dynamic actions in the postcritical regime lead to completely different load-displacement curves. This must be taken into account while interpreting results of purely static analyses.

Buckling and snap-through can be regarded as archetypes of nonlinear behavior of shells in the sense that each deformation process can be viewed as a combination of both. The dominance of one or the other mechanism has some impact on related solution methods. For instance, linear eigenvalue analysis may serve as a method for the approximate determination of a linear buckling load (provided nonlinearities in the prebuckling path are sufficiently small), whereas the same technique is practically useless in the case of snap-through problems, unless several accompanying eigenvalue analyses during the loading process eventually identify the limit load (Helnwein, 1998).

4 DIMENSIONAL REDUCTION AND STRUCTURAL MODELS

In nonpolar *continuum* theory – not focusing on specific structures – mechanical modeling exclusively concerns the constitutive law. Specific choices of strain measures, time integration algorithms, finite element formulations, or spatial discretization may have considerable impact on

numerical behavior and approximation quality. However, the *exact* solution of a *continuous* initial boundary-value problem only differs if a different constitutive law is applied. This does not only include solid mechanics but general continua, for instance, fluids, for which the kinematic equations, equilibrium, balance of mass, and momentum, and so on, are identical.

The notion of a *structural model* comes into play as soon as information about geometry or fabrication properties of a certain class of structures are used for an a priori modification of the three-dimensional equations. In the context of thin-walled structures like plates and shells, these modifications consist in dimensional reduction from three to two dimensions. Different techniques to obtain such models are outlined in Sections 4.1–4.3. The respective model assumptions are addressed in Section 4.4.

Historically, structural models have been developed to simplify the governing differential equations in order to make a certain class of problems accessible to analytical – exact or approximate – solution methods, impossible to apply in the three-dimensional case due to the complexity of the equations, mostly because of the boundary conditions. In many cases, such models are inspired by a sophisticated insight into the structural behavior, rather than being obtained from an analytical dimensional reduction. The ingenious assumption, commonly attributed to Leonhard Euler and Jakob Bernoulli, of initially straight cross sections remaining straight throughout deformation is a classical example for this. Often, such reduced models have been established ab initio without making use of (or even having available) the underlying three-dimensional equations.

These models are indispensable in all fields of structural engineering and consequently, related computational strategies have been developed during the advent of finite elements methods. While there is no need to simplify differential equations when a weak form is used to construct approximate solutions, application of structural models instead of the complete three-dimensional theory in the context of finite element analysis still includes the advantage of saving degrees of freedom and thus computing time. A second, not less important, advantage of the dimensional reduction is condensation of the three-dimensional response and the related mechanical insight into typical ‘engineering phenomena’, like stretching, transverse shear deformation, bending, or twisting.

Given the continuing developments in the computer industry and the seemingly unlimited progress in computational power, one might argue that these advantages are becoming more and more obsolete. There is, however, much more to the models developed by our ancestors than merely reducing the number of unknowns in an abstract

mathematical theory. Structural models effectively reproduce the substantial aspects of real mechanical behavior, observed in experiments, while omitting subsidiary effects. As an example, take the stress distribution of a clamped plate under uniform load. The exact solution according to three-dimensional theory of elasticity yields singularities in the stress distribution near the edges and one has to take into account nonlinear constitutive models, like elastoplasticity or damage, in order to obtain realistic results. A simple, linear-elastic Kirchhoff plate theory, however, renders approximate results that match experimental evidence quite well, even when a simple linear material model is used. We may conclude that structural models are more than just simplifications of a three-dimensional theory. Nevertheless, it is sensible to take the three-dimensional equations as a reference for quantification of the influence of certain simplifications, which is what we will do in Section 4.4.

Historically, the first plate and shell models have been developed heuristically, for instance, on the basis of Euler’s and Bernoulli’s assumptions mentioned above. Later, these models have been provided with a mathematical basis by comparison with the exact three-dimensional equations by means of *asymptotic analysis* (Morgenstern, 1959; Friedrichs and Dressler, 1961; Gol’denveizer and Kolos, 1965; Dauge and Gruais, 1996; Arnold and Falk, 1996; Paumier and Raoult, 1997, see also Ciarlet, 1990 and **Chapter 8 of Volume 1** for an overview). A plate or shell model is said to be *asymptotically correct* if the model solution converges toward the three-dimensional solution in the limit of vanishing thickness. It was, for instance, not before one century later that Kirchhoff’s plate theory from 1850, Kirchhoff (1850), has been justified mathematically by Morgenstern (1959), who proved its asymptotic correctness.

It is important to remark that the error in the thin limit has to be estimated by specifically designed measures in order to obtain convergence. In general situations, the model solution will not reproduce the three-dimensional one exactly at each location in space (a simple example is the aforementioned singularities, which do not vanish in the thin limit).

It turns out that a certain balance between through-the-thickness distribution of strains and stresses is crucial for the resulting model to be asymptotically correct (Libai and Simmonds, 1998), necessitating a modification of the material law for lower order models.

Developing plate and shell models essentially constitutes a spatial *semidiscretization* of the continuous problem. There is an immense number of different models, a mere enumeration of which does not make sense. We will therefore focus on description of principle strategies to realize dimensional reduction (Sections 4.1–4.3) as

well as the related assumptions (Section 4.4). It will turn out that apparently different philosophies – deriving shell theories from three-dimensional continuum mechanics, Section 4.1, directly establishing two-dimensional equations, Section 4.2, or developing finite shell elements by ‘degenerating’ solid elements, Section 4.3 – are in fact identical if the same model assumptions are made.

Conceptually, however, derivation from the three-dimensional continuum equations is probably the most general approach because it naturally includes arbitrarily complex models, including hierarchic higher-order models or layer-wise theories, useful for computation of composites and laminates.

Throughout Section 4.4, we will specialize the mentioned model decisions and discretization to a standard conventional *5-parameter shell model with Reissner–Mindlin kinematics*. This means that five independent variables, namely, three midsurface displacements and two independent rotations are used for parameterization of displacements. Thus, as rotations are independent of the gradients of the midsurface, this model allows for transverse shear deformations, a feature that is commonly associated with the names of Reissner and Mindlin (Reissner, 1945; Mindlin, 1951). Like this paragraph, the corresponding parts of the text are set within a frame for easy identification.

4.1 Derivation from three-dimensional continuum

A natural way to look at models or theories for thin-walled structures is their interpretation as a certain approximation of the three-dimensional equations. We will refer to the three-dimensional theory of *elasticity* in most parts of this text. This, however, does not mean that the described concepts are restricted to elasticity problems; they are equally well suited to treat problems involving plasticity, damage or other kinds of material nonlinearities.

The modus operandi to obtain a reduced model from the three-dimensional equations unfolding in what follows focuses on shells, but it is applicable to beams and plates as well. While plates can be viewed as a special case of shells, the modifications to obtain general beam formulations are more complex, since dimensional reduction reduces the three-dimensional continuum to a one-dimensional structure. Here, in particular, torsion introduces some complexity.

The original development of the direct approach is mostly attributed to Ericksen and Truesdell (1958). An excellent and exhaustive treatise on the subject has been given by Naghdi (1972). Without exactly reproducing the details of his derivations, the principal concept is described in the following.

The starting point is the parameterization of the three-dimensional shell body by curvilinear coordinate lines θ^i , thus specifying in-plane (θ^1, θ^2) and transverse (θ^3) directions, as already introduced in Section 2. Without loss of generality, we may assume at this point that θ^3 is orthogonal to θ^1 and θ^2 . This facilitates the representation of an arbitrary position vector in the deformed configuration within the shell body as an infinite sum of functions of the in-plane coordinates

$$\mathbf{x}(\theta^1, \theta^2, \theta^3) = \sum_{N=0}^{\infty} (\theta^3)^N \mathbf{r}^N(\theta^1, \theta^2) \quad (54)$$

Here, \mathbf{r}^0 denotes the position vector to the midsurface, the other \mathbf{r}^N can be interpreted as directors pointing into three-dimensional shell space. Note that the N in $(\theta^3)^N$ indicates an exponent while in \mathbf{r}^N , it has to be understood as a superscript. For the undeformed configuration, a similar or a simplified description may be chosen (the latter, if the higher terms are not needed in the geometric description of the undeformed shell structure):

$$\mathbf{X}(\theta^1, \theta^2, \theta^3) = \sum_{N=0}^{\infty} (\theta^3)^N \mathbf{R}^N(\theta^1, \theta^2) \quad (55)$$

or, for the simplified version,

$$\mathbf{X}(\theta^1, \theta^2, \theta^3) = \mathbf{R}^0(\theta^1, \theta^2) + \theta^3 \mathbf{R}^1(\theta^1, \theta^2) \quad (56)$$

Here, $\mathbf{r}^0, \mathbf{r}^1, \mathbf{r}^2, \dots$ and $\mathbf{R}^0, \mathbf{R}^1, \mathbf{R}^2, \dots$, respectively, are three-dimensional, vector-valued functions of the in-plane coordinates. As the sum incorporates an infinite number of components, this means that the underlying shell model contains an infinite number of parameters or degrees of freedom. The displacements $\mathbf{u} = \mathbf{x} - \mathbf{X}$ are given by

$$\mathbf{u}(\theta^1, \theta^2, \theta^3) = \sum_{N=0}^{\infty} (\theta^3)^N \mathbf{v}^N(\theta^1, \theta^2) \quad (57)$$

Likewise, we are expanding the body forces

$$\rho \mathbf{b}(\theta^1, \theta^2, \theta^3) = \sum_{N=0}^{\infty} (\theta^3)^N \rho \mathbf{b}^N(\theta^1, \theta^2) \quad (58)$$

Within this framework, a particular shell model can be specified by restricting the sum to a finite number N_u of components,

$$\mathbf{u}(\theta^1, \theta^2, \theta^3) \approx \sum_{N=0}^{N_u} (\theta^3)^N \mathbf{v}^N(\theta^1, \theta^2) \quad (59)$$

The same expansions hold for \mathbf{x} , \mathbf{X} and $\rho\mathbf{b}$,

$$\begin{aligned}\mathbf{x} &\approx \sum_{N=0}^{N_x} (\theta^3)^N \mathbf{r}^N, & \mathbf{X} &\approx \sum_{N=0}^{N_x} (\theta^3)^N \mathbf{R}^N, \\ \rho\mathbf{b} &\approx \sum_{N=0}^{N_b} (\theta^3)^N \rho\mathbf{b}^N\end{aligned}\quad (60)$$

where $N_x = \max\{N_u, N_X\}$.

The approximation of the displacement field $\mathbf{u}(\theta^i)$ established in equation (59) can be interpreted as a semidiscretization of the three-dimensional continuum in one spatial dimension, namely, the transverse direction θ^3 . The corresponding shape functions are the monomials $(\theta^3)^N$ and the parameters (degrees of freedom) \mathbf{v}^N are functions of the in-plane coordinates θ^1, θ^2 . In order to accomplish a certain balance between in-plane and transverse strain distribution, the displacement expansion (59) may be supplemented by additional conditions, like inextensibility of the director $\mathbf{R}^1 = \mathbf{D}$ (cf. equation (17)), in the case of Kirchhoff–Love and Reissner–Mindlin-type models.

It may also be sensible to choose different orders of approximation for in-plane and transverse displacements. In order to avoid an awkward notation, we are not attempting to cast all possible parameterizations of the through-the-thickness distribution of the displacements into a general formal framework. Specific models of this kind are put into more concrete terms in Section 4.4.

The unknowns represent displacements, or generalized displacements, like rotations, cross-sectional warping, and so on, in the above-mentioned semidiscretization on the basis of the virtual work principle. Similar to finite element formulations, alternative multifield variational approaches could be utilized as well. For instance, the shell models proposed by Büchter and Ramm (1992a) (see also Büchter, Ramm and Roehl, 1994; Betsch, Gruttmann and Stein, 1995; Bischoff and Ramm, 1997, among many others), based on the *enhanced assumed strain (EAS)* method (Simo and Rifai, 1990) following a modified version of the Hu–Washizu principle, can be assigned to this group. If strains and stresses are used as free variables, the classical concept of *intrinsic* shell theories is recovered.

The monomials used as shape functions used in equation (59) represent just one out of numerous possibilities. The shape functions neither have to be monomials nor do they need to satisfy more than C^0 -continuity, that is, for instance, a layer-wise linear approach is possible as well. The most important models are described later in Section 4.5.

The derivation of strains and stresses is straightforward in the sense that the standard equations of the three-dimensional theory are applied. For first-order models with

linear approximation of transverse displacements, additional measures have to be taken in order to obtain an asymptotically correct theory. The most general way is to modify the material equations by explicitly setting transverse normal stresses to zero (see Section 4.4.5).

An expression for the curvilinear components of the Green–Lagrange strain tensor has been given in equation (37) and is reproduced here for convenience,

$$\begin{aligned}\mathbf{E} &= E_{ij} \mathbf{G}^i \otimes \mathbf{G}^j, \\ E_{ij} &= \frac{1}{2} (\mathbf{u}_{,i} \cdot \mathbf{G}_j + \mathbf{u}_{,j} \cdot \mathbf{G}_i + \mathbf{u}_{,i} \cdot \mathbf{u}_{,j})\end{aligned}$$

The covariant base vectors are

$$\mathbf{G}_\alpha = \sum_{N=0}^{N_x} (\theta^3)^N \mathbf{R}_{,\alpha}^N, \quad \mathbf{G}_3 = \sum_{N=0}^{N_x} N (\theta^3)^{N-1} \mathbf{R}^N \quad (61)$$

and the derivatives of the displacement vectors read

$$\mathbf{u}_{,\alpha} = \sum_{N=0}^{N_x} (\theta^3)^N \mathbf{v}_{,\alpha}^N, \quad \mathbf{u}_{,3} = \sum_{N=0}^{N_x} N (\theta^3)^{N-1} \mathbf{v}^N \quad (62)$$

Substituting equations (61) and (62) into (37) provides a general expression for the strains in terms of the parameterization of the shell geometry \mathbf{R}^N and the degrees of freedom \mathbf{v}^N . The resulting lengthy expressions are not reproduced here, but put into concrete terms later in Section 4.4 for specific models.

For general shells, the actual metric has to be mapped from an arbitrary point in the shell body onto the midsurface, which is accomplished with the help of a second-order tensor

$$\mathbf{Z} := \mathbf{G}^i \otimes \mathbf{A}_i \quad (63)$$

sometimes called the *shifter tensor* or *shell shifter*. Its definition resembles that of the deformation gradient, equation (32), and in fact \mathbf{Z} accomplishes nothing else than a map from one configuration space to another, here from the shell body to its midsurface,

$$\mathbf{G}^i = \mathbf{Z} \cdot \mathbf{A}^i, \quad \mathbf{G}_i = \mathbf{Z}^{-1} \cdot \mathbf{A}_i \quad (64)$$

The relationship between the three-dimensional strain tensor \mathbf{E} and the strain tensor $\hat{\mathbf{E}}$ referring to the midsurface of the shell is

$$\mathbf{E} = \mathbf{Z} \cdot \hat{\mathbf{E}} \cdot \mathbf{Z}^T, \quad \hat{\mathbf{E}} = E_{ij} \mathbf{A}^i \otimes \mathbf{A}^j = \mathbf{Z}^{-1} \cdot \mathbf{E} \cdot \mathbf{Z}^{-T} \quad (65)$$

Note that for curved shells in general, $\mathbf{E} \neq \hat{\mathbf{E}}$, although we are using the same *components* E_{ij} .

It may seem more natural to express the original strain tensor \mathbf{E} in terms of alternative strain components \hat{E}_{ij} referring to the metric of the midsurface via

$$\begin{aligned} \mathbf{E} &= E_{ij} \mathbf{G}^i \otimes \mathbf{G}^j =: \hat{E}_{ij} \mathbf{A}^i \otimes \mathbf{A}^j \\ \Rightarrow \hat{E}_{ij} &= E_{kl} (\mathbf{G}^k \cdot \mathbf{A}_i) (\mathbf{G}^l \cdot \mathbf{A}_j) \end{aligned} \quad (66)$$

However, the contravariant base vectors contained in the expression for \hat{E}_{ij} involve fractions of rational functions of the thickness coordinate θ^3 and consequently, subdivision of the strain components into functions that are constant, linear, and so on with respect to θ^3 is impossible, thus precluding a convenient and physically meaningful definition of strain measures like membrane strains, curvature changes, and so on.

It turns out that the highest polynomial order with respect to the thickness coordinate showing up in the expression for the strain components E_{ij} is N_x^2 . Consequently, the strain distributions can be written as

$$E_{kl} = \sum_{N=0}^{N_x^2} (\theta^3)^N E_{kl}^N \quad (67)$$

where the E_{kl}^N immediately follow from substituting equations (61) and (62) into (37). It will be demonstrated in the following how this leads quite naturally to the concept of strain measures, like membrane strains and curvatures changes, and stress resultants, like membrane forces and bending moments. Of course, it is also possible to define stress resultants ad hoc and establish a corresponding material law afterwards.

Analogous to the definition of $\hat{\mathbf{E}}$, equation (65), we define a modified stress tensor $\hat{\mathbf{S}}$ by

$$\mathbf{S} = \mathbf{Z}^{-T} \cdot \hat{\mathbf{S}} \cdot \mathbf{Z}^{-1} \Rightarrow \hat{\mathbf{S}} = \mathbf{Z}^T \cdot \mathbf{S} \cdot \mathbf{Z} = S^{ij} \mathbf{A}_i \otimes \mathbf{A}_j \quad (68)$$

It is shown in the appendix that $\hat{\mathbf{S}}$ and $\hat{\mathbf{E}}$ are energetically conjugate, and

$$\mathbf{E}^T : \mathbf{S} = \hat{\mathbf{E}}^T : \hat{\mathbf{S}} \quad (69)$$

The transformation rule for $\hat{\mathbf{S}}$ and \mathbf{S} differs from the one for the strains in equation (65) because contravariant components are used for representation of the stress tensor.

In view of finite element formulations, we will refrain from the cumbersome derivation of the governing differential equations in terms of equilibrium conditions and directly proceed to the corresponding expressions for internal and external energy emanating from strains, stresses, body forces, and displacements.

A thorough treatment of displacement and force boundary conditions for arbitrarily curved shell boundaries is also

omitted here for the sake of simplicity and because it is not needed for understanding the essentials of the shell models discussed herein.

The material law corresponding to $\hat{\mathbf{E}}$ and $\hat{\mathbf{S}}$ (cf. equation (41)) is

$$\hat{\mathbf{S}} = \hat{\mathbf{C}} : \hat{\mathbf{E}} \quad (70)$$

where

$$\hat{\mathbf{C}} = C^{ijkl} \mathbf{A}_i \otimes \mathbf{A}_j \otimes \mathbf{A}_k \otimes \mathbf{A}_l \quad (71)$$

Derivation of equation (70), confirming (71), can be found in the appendix.

The expression for the internal virtual work (cf. equation (51)) then reads

$$\begin{aligned} -\delta \Pi^{\text{int}} &= \int_{\Omega} \delta \hat{\mathbf{E}} : \hat{\mathbf{C}} : \hat{\mathbf{E}} \, d\Omega = \int_{\Omega} \delta E_{ij} C^{ijkl} E_{kl} \, d\Omega \\ &= \int_{\Omega^0} \int_{-(t/2)}^{t/2} \delta E_{ij} C^{ijkl} E_{kl} Z \, d\theta^3 \, d\Omega^0 \end{aligned} \quad (72)$$

where Ω^0 stands for the middle surface of the shell body Ω and

$$Z = \text{Det}(\mathbf{Z}^{-1}) = \frac{(\mathbf{G}_1 \times \mathbf{G}_2) \cdot \mathbf{G}_3}{\|\mathbf{A}_1 \times \mathbf{A}_2\|} \quad (73)$$

is the absolute value of the inverse of the shell shifter, equation (63). Z establishes decomposition of an infinitesimal volume element into contributions from midsurface and thickness direction. Shell thickness t may be a function of the in-plane coordinates θ^1, θ^2 , cf. equation (15).

The required variation of $\hat{\mathbf{E}}$ and its components, respectively, is given by

$$\delta \hat{\mathbf{E}} = \frac{\partial \hat{\mathbf{E}}}{\partial \mathbf{u}} \cdot \delta \mathbf{u}, \quad \delta E_{ij} = \frac{\partial E_{ij}}{\partial u_k} \delta u_k \quad (74)$$

The external virtual work is

$$\begin{aligned} \delta \Pi^{\text{ext}} &= \int_{\Omega} \rho \mathbf{b} \cdot \delta \mathbf{u} \, d\Omega = \int_{\Omega} \rho b^i \delta u_i \, d\Omega \\ &= \int_{\Omega^0} \int_{-(t/2)}^{t/2} \rho b^i \delta u_i Z \, d\theta^3 \, d\Omega^0 \end{aligned} \quad (75)$$

where the components of \mathbf{b} and $\delta \mathbf{u}$ may simply refer to a Cartesian frame.

Development of a certain shell theory will eventually lead to a two-dimensional formulation with all the involved variables being defined on the midsurface, expressed as functions of the in-plane coordinates θ^1 and θ^2 . To this end, the integral in θ^3 -direction has to be evaluated in

advance (more details on thickness integration are found in Section 4.4.6). Introducing equation (67) into (72) yields

$$\begin{aligned}
 -\delta\Pi^{\text{int}} &= \int_{\Omega^0} \int_{-(t/2)}^{t/2} \sum_{N=0}^{N_x^2} (\theta^3)^N \delta E_{ij}^N C^{ijkl} \\
 &\quad \cdots \sum_{M=0}^{N_x^2} (\theta^3)^M E_{kl}^M Z \, d\theta^3 \, d\Omega^0 = \int_{\Omega^0} \sum_{N=0}^{N_x^2} \sum_{M=0}^{N_x^2} \delta E_{ij}^N \\
 &\quad \cdots \int_{-(t/2)}^{t/2} (\theta^3)^N C^{ijkl} (\theta^3)^M Z \, d\theta^3 E_{kl}^M \, d\Omega^0 \\
 &= \int_{\Omega^0} \sum_{N=0}^{N_x^2} \sum_{M=0}^{N_x^2} \delta E_{ij}^N D_{N+M}^{ijkl} E_{kl}^M \, d\Omega^0 \quad (76)
 \end{aligned}$$

where

$$D_K^{ijkl} = \int_{-(t/2)}^{t/2} (\theta^3)^K C^{ijkl} Z \, d\theta^3 \quad (77)$$

represents the material matrix of the shell model. Likewise,

$$\begin{aligned}
 \delta\Pi^{\text{ext}} &= \int_{\Omega^0} \int_{-(t/2)}^{t/2} \rho \sum_{N=0}^{N_b} (\theta^3)^N b_N^i \sum_{M=0}^{N_u} (\theta^3)^M \delta u_i^M Z \, d\theta^3 \, d\Omega^0 \\
 &= \int_{\Omega^0} \int_{-(t/2)}^{t/2} \rho \sum_{N=0}^{N_b} \sum_{M=0}^{N_u} (\theta^3)^{N+M} Z \, d\theta^3 b_N^i \delta u_i^M \, d\Omega^0 \quad (78)
 \end{aligned}$$

Preintegration of the material law directly implies the definition of energetically conjugate quantities

$$\hat{\mathbf{n}}_M := n_M^{ij} \mathbf{A}_i \otimes \mathbf{A}_j \quad (79)$$

to the strain variables, with

$$\begin{aligned}
 n_M^{ij} &:= \int_{-(t/2)}^{t/2} (\theta^3)^M S^{ij} Z \, d\theta^3 = \int_{-(t/2)}^{t/2} (\theta^3)^M C^{ijkl} E_{kl} Z \, d\theta^3 \\
 &= \int_{-(t/2)}^{t/2} (\theta^3)^M C^{ijkl} \sum_{N=0}^{N_x^2} (\theta^3)^N E_{kl}^N Z \, d\theta^3 \\
 &= \sum_{N=0}^{N_x^2} \int_{-(t/2)}^{t/2} (\theta^3)^{N+M} C^{ijkl} Z \, d\theta^3 E_{kl}^N = \sum_{N=0}^{N_x^2} D_{N+M}^{ijkl} E_{kl}^N \quad (80)
 \end{aligned}$$

Here, we have made use of equations (47), (67), and (77) for the individual steps. The notation $\hat{\mathbf{n}}_M$ (instead of \mathbf{n}_M) in equation (79) is justified because the components n_M^{ij} refer to the midsurface metric, just like in $\hat{\mathbf{S}}$.

The second-order tensor $\hat{\mathbf{n}}_M$ does *not* represent the ‘real’ stress resultants that are accessible to direct physical interpretation, because their definition is based on the second

Piola–Kirchhoff stress tensor, being defined on the reference configuration. Its components n_M^{ij} merely represent the energetically conjugate variables to the strain variables E_{ij}^M , such that

$$-\delta\Pi^{\text{int}} = \int_{\Omega^0} \sum_{M=0}^{N_x^2} n_M^{kl} \delta E_{kl}^M \, d\Omega^0 \quad (81)$$

Without explicit derivation, the physically relevant *real stress resultants*, based on the Cauchy stress tensor $\boldsymbol{\sigma}$ are given by

$$N_0 = \int_{-(t/2)}^{t/2} \boldsymbol{\sigma} \cdot \mathbf{z} \, z \, d\theta^3, \quad N_1 = \int_{-(t/2)}^{t/2} \theta^3 \boldsymbol{\sigma} \cdot \mathbf{z} \, z \, d\theta^3 \quad (82)$$

where

$$\mathbf{z} := \mathbf{g}^i \otimes \mathbf{a}_i \quad (83)$$

is the shifter in the current configuration, and $z = \text{Det}(\mathbf{z}^{-1})$ denotes the determinant of its inverse. N_0 corresponds to the linear part of through-the-thickness stress distribution and thus contains the resulting membrane and shear forces. N_1 represents the linear part of $\boldsymbol{\sigma}$ in θ^3 and thus contains the resulting bending and twisting moments. Note that in the given general context, N_0 and N_1 do also contain the integrals of transverse normal stresses, which are not *resultant* forces but merely abstract stress integrals (Bischoff and Ramm, 2000). The definition of higher-order stress resultants is possible but requires additional considerations concerning orthogonality of the shape functions used for expansion of strains and stresses in thickness direction.

The definition of stress resultants completes dimensional reduction of the three-dimensional equations. Strain measures E_{kl}^N , stress resultants n_M^{ij} (N_m , respectively), and the corresponding components of the material tensor D_{N+M}^{ijkl} are known functions of midsurface quantities only.

The underlying equations are still *exactly* equivalent to the three-dimensional formulation in the limit of $\{N_x, N_u, N_b\} \rightarrow \infty$. Moreover, for a *given* three-dimensional displacement field with finite $\{N_x, N_u, N_b\}$, the resulting strains and stresses as well as the internal and external energies are exact as well, in contrast to the geometrically exact formulation derived in the following section. This somewhat academic argument will be of some importance later in Section 4.4.

Approximations come into the picture as soon as the sums describing geometry, load, and displacements are restricted to a finite number of components, neglecting higher-order terms. Further assumptions affect through-the-thickness distribution of strains and stresses, the material law as well as its preintegration and certain approximations of the shifter \mathbf{Z} . The bottom line of this concept is that

the deformation of the three-dimensional shell body is approximated by carefully chosen functions of the thickness coordinate θ^3 .

4.2 Direct approach

The principal idea of the direct approach can be traced back to the theory of the brothers Cosserat and Cosserat (1909) who proposed an extension of the classical continuum, introducing rotations to a material point as additional degrees of freedom. The concept, also known as *micropolar theory*, has been picked up in the 1950/1960s for different applications and also utilized in an elegant way to model the rotations of the cross sections for thin-walled structures, represented as a two-dimensional surface enhanced by directors. For an extensive discussion, confer Rubin (2000).

Shell models of this group are also often denoted as *geometrically exact* (Simo and Fox, 1989), but this does not mean that the approximation of the actual three-dimensional geometry of the deformed shell structure is necessarily more accurate than in other models. It merely reflects the fact that the concept is not derived from geometric approximations of a three-dimensional body but starts from an *exact* kinematic description of a two-dimensional Cosserat surface. Moreover, it does not introduce any restrictions with respect to the size of rotations (cf. Section 4.4.7). The crucial model assumptions are thus concentrated in the constitutive equations, that is, three-dimensional theory of elasticity comes into play while defining the material law.

Apparently, there is no unique definition of what a ‘geometrically exact’ model would be. In the present article, we follow the concept introduced by Juan Simo and coworkers, where the geometrically exact approach is confronted with the so-called degenerated solid approach, treated in the next section. Accordingly, the only difference is in the way reduction to resultant form – and thus through-the-thickness integration – is accomplished (analytical through-the-thickness integration in the former and numerical quadrature in the latter). In this sense, the geometrically exact approach in the context of finite element analysis may well be understood as being based on classical shell theory.

In contrast to the previous section, in which shell equations are obtained by a systematic dimensional reduction neglecting higher-order terms, in the present framework, the governing equations are merely postulated. Of course, this is done with the intention to comply with mechanically sensible assumptions in order to obtain an asymptotically correct theory.

As in the previous section, the shell theory unfolds on the basis of kinematic (geometric) considerations. From

a general perspective, this concept describes a directed continuum in which the placement of a material point is specified not only by its position vector, but additionally, by a set of directors associated with each material point. In the present case, an *inextensible one-director Cosserat surface* is utilized.

Mathematically, the kinematic description of the shell represents a differentiable manifold

$$\mathcal{C} = \{(\mathbf{r}, \mathbf{d}) : \mathcal{A} \subset \mathbb{R}^2 \rightarrow \mathbb{R}^3 \times \mathcal{S}^2\} \quad (84)$$

where \mathcal{S}^2 is defined as the unit sphere

$$\mathcal{S}^2 = \{\mathbf{d} \in \mathbb{R}^3 : \|\mathbf{d}\| = 1\} \quad (85)$$

$\|\circ\|$ being the Euclidean norm in \mathbb{R}^3 (cf. equation (5)).

Unlike the three-dimensional configuration space used in continuum mechanics, \mathcal{C} is not a linear space, because its representation contains the nonlinear manifold \mathcal{S}^2 . We will see in the following that this introduces certain peculiarities in the parameterization of the deformation, in particular, the rotations needed for the director update.

The parameter space $\mathcal{A} \subset \mathbb{R}^2$ is an open set, representing the middle surface of the shell. We shall assume for the subsequent derivations that it has a sufficiently smooth boundary $\partial\mathcal{A}$. The closure of \mathcal{A} is referred to as $\overline{\mathcal{A}} = \mathcal{A} \cup \partial\mathcal{A}$. \mathbb{R}^2 and \mathbb{R}^3 represent the usual real-valued two- and three-space, respectively.

The essence of equation (84) is that $\mathbf{r} : \mathcal{A} \rightarrow \mathbb{R}^3$ maps points of the shell’s parameter space into three-dimensional space, thus describing the deformation of its middle surface and $\mathbf{d} : \mathcal{A} \rightarrow \mathcal{S}^2$ correlates a director with each point of the midsurface.

Within this framework, the reference configuration of the shell can be written as

$$\mathfrak{S}_0 := \left\{ \mathbf{X} \in \mathbb{R}^3 : \mathbf{X} = \mathbf{R} + \theta^3 \mathbf{D} \right. \\ \left. \text{with } (\mathbf{R}, \mathbf{D}) \in \mathcal{C} \text{ and } \theta^3 \in \left[-\frac{t}{2}, \frac{t}{2} \right] \right\} \quad (86)$$

The deformed, or current configuration is

$$\mathfrak{S} := \left\{ \mathbf{x} \in \mathbb{R}^3 : \mathbf{x} = \mathbf{r} + \theta^3 \mathbf{d} \right. \\ \left. \text{with } (\mathbf{r}, \mathbf{d}) \in \mathcal{C} \text{ and } \theta^3 \in \left[-\frac{t}{2}, \frac{t}{2} \right] \right\} \quad (87)$$

The kinematic assumptions associated with the map $\Phi : \mathfrak{S}_0 \rightarrow \mathfrak{S}$ are identical to that of a shear deformable first-order theory, assuming initially straight cross-sectional fibers remaining straight and unstretched throughout deformation, allowing for transverse shear strains and neglecting

thickness change. Moreover, initial shell thickness t is assumed to be constant with respect to θ^α . A similar model can be obtained from the concept described in the previous section by appropriate assumptions for displacements and geometry.

The principal concept, however, is not restricted to this model but rather general. Given appropriate definitions of \mathcal{C} , the same multitude of models as described in the previous section can be derived (see, for instance, Simo, Rifai and Fox (1990) for a formulation including through-the-thickness stretching).

A crucial point in the development of geometrically exact shell formulations is parameterization of the rotations. We dedicate a good part of Section 5.3 to this topic and therefore postpone provision of the underlying mathematical definitions to this section. The remarks therein are also valid in the context of continuum-based shell elements. For the time being, we take for granted that a unique parameterization of a rotation tensor $\mathbf{A} \in S_D^2 \subset SO(3)$ is at hand (assuming smooth shells). The corresponding rotation vector Θ is uniquely specified by two independent parameters and maps the director from the undeformed (reference) configuration onto the deformed (current) configuration,

$$\mathbf{d} = \mathbf{A} \cdot \mathbf{D} \quad (88)$$

without introducing drilling around the director \mathbf{D} . Moreover, we assume in the following that $\mathbf{D} = \mathbf{A}_3$ (cf. equation (17)), that is, the director field is orthogonal to the midsurface of the shell. For smooth shells, this can be done without loss of generality for the resulting shell theory. In the case of a discretization method, however, the question of orthogonality of the director field reenters the focus of interest. As this is a question of discretization rather than theory, this is discussed in more detail in Section 5.2.

The displacement of any arbitrary point in the shell body is given as

$$\mathbf{u} := \mathbf{x} - \mathbf{X} = \mathbf{r} + \theta^3 \mathbf{d} - \mathbf{R} - \theta^3 \mathbf{D} \quad (89)$$

With the displacements of the midsurface

$$\mathbf{v} := \mathbf{r} - \mathbf{R} \quad (90)$$

and the previously defined rotation tensor \mathbf{A} , we obtain the typical parameterization of a shear deformable 5-parameter shell model with Reissner–Mindlin kinematics,

$$\mathbf{r} = \mathbf{R} + \mathbf{v}, \quad \mathbf{d} = \mathbf{A} \cdot \mathbf{D} \quad (91)$$

$$\mathbf{v} = v^i \mathbf{e}_i, \quad \mathbf{A} \in S_D^2, \quad \Theta = \Theta^\alpha \mathbf{A}_\alpha \quad (92)$$

$$\rightarrow \mathbf{u} = \mathbf{v} + \theta^3 (\mathbf{A} - \mathbf{G}) \cdot \mathbf{D} \quad (93)$$

The free variables are the three components v^i of the midsurface displacements along with two rotations Θ^α .

Next, we define strain variables such that

$$\begin{aligned} \mathbf{E} = E_{ij} \mathbf{G}^i \otimes \mathbf{G}^j =: & (\varepsilon_{\alpha\beta} + \theta^3 \kappa_{\alpha\beta} + (\theta^3)^2 \chi_{\alpha\beta}) \mathbf{G}^\alpha \otimes \mathbf{G}^\beta \\ & + \gamma_\alpha \frac{1}{2} (\mathbf{G}^\alpha \otimes \mathbf{G}^3 + \mathbf{G}^3 \otimes \mathbf{G}^\alpha) \end{aligned} \quad (94)$$

with E_{ij} defined according to equation (37). Expressing the covariant base vectors in terms of the metric on the midsurface

$$\mathbf{G}_\alpha = \mathbf{A}_\alpha + \theta^3 \mathbf{A}_{3,\alpha}, \quad \mathbf{G}_3 = \mathbf{A}_3 \quad (95)$$

$$\mathbf{g}_\alpha = \mathbf{a}_\alpha + \theta^3 \mathbf{a}_{3,\alpha}, \quad \mathbf{g}_3 = \mathbf{a}_3 \quad (96)$$

we can write

$$\begin{aligned} E_{\alpha\beta} = & \frac{1}{2} (a_{\alpha\beta} + 2\theta^3 b_{\alpha\beta} + (\theta^3)^2 \mathbf{a}_{3,\alpha} \cdot \mathbf{a}_{3,\beta} \\ & - A_{\alpha\beta} - 2\theta^3 B_{\alpha\beta} - (\theta^3)^2 \mathbf{A}_{3,\alpha} \cdot \mathbf{A}_{3,\beta}) \end{aligned} \quad (97)$$

$$\begin{aligned} E_{\alpha 3} = & \frac{1}{2} (a_{\alpha 3} + \theta^3 \mathbf{a}_{3,\alpha} \cdot \mathbf{a}_3 - A_{\alpha 3} - \theta^3 \mathbf{A}_{3,\alpha} \cdot \mathbf{A}_3) \\ = & \frac{1}{2} (a_{\alpha 3} - A_{\alpha 3}) \end{aligned} \quad (98)$$

$$E_{33} = 0 \quad (99)$$

The quadratic terms with respect to θ^3 in equation (97) are usually neglected, which is justified for thin shells, as well as in the case of moderately thick shells if the bending deformations are small (see Section 4.4.3 for a discussion of strain assumptions). The fact that $\mathbf{a}_{3,\alpha} \cdot \mathbf{a}_3 - \mathbf{A}_{3,\alpha} \cdot \mathbf{A}_3 = 0$, used in equation (98) to eliminate the linear part of the transverse shear strains, is not an approximation but holds exactly due to inextensibility of the director (see appendix for a proof).

On the basis of these definitions, we obtain expressions for membrane strains

$$\boldsymbol{\varepsilon} = \varepsilon_{\alpha\beta} \mathbf{A}^\alpha \otimes \mathbf{A}^\beta, \quad \varepsilon_{\alpha\beta} = \frac{1}{2} (a_{\alpha\beta} - A_{\alpha\beta}) \quad (100)$$

curvatures and twist

$$\boldsymbol{\kappa} = \kappa_{\alpha\beta} \mathbf{A}^\alpha \otimes \mathbf{A}^\beta, \quad \kappa_{\alpha\beta} = b_{\alpha\beta} - B_{\alpha\beta} \quad (101)$$

as well as transverse shear strains

$$\boldsymbol{\gamma} = \gamma_\alpha \mathbf{A}^\alpha, \quad \gamma_\alpha = a_{\alpha 3} - A_{\alpha 3} \quad (102)$$

Note that the tensor components in equations (100)–(102) refer to base vectors \mathbf{A}^α of the midsurface, as opposed to E_{ij} referring to \mathbf{G}^i . Again, this does not introduce any sort of approximation, it only has an impact on the physical interpretation of the strain variables $\boldsymbol{\varepsilon}$, $\boldsymbol{\kappa}$, and $\boldsymbol{\gamma}$. For the

same reason, the expression for the three-dimensional strain state at an arbitrary point in the shell in terms of these strain variables

$$\mathbf{E} = \mathbf{Z} \cdot (\boldsymbol{\varepsilon} + \theta^3 \boldsymbol{\kappa}) \cdot \mathbf{Z}^T + \frac{1}{2} [(\boldsymbol{\gamma} \cdot \mathbf{Z}^T) \otimes \mathbf{A}^3 + \mathbf{A}^3 \otimes (\mathbf{Z} \cdot \boldsymbol{\gamma})] \quad (103)$$

contains the shifter \mathbf{Z} , realizing the map from the midsurface into shell space. The aforementioned simplification, namely, neglecting quadratic terms in the thickness coordinate θ^3 , has been taken into account in equation (103).

Comparing equation (103) above and equation (65) in the previous section reveals that there is a strong relationship between $\boldsymbol{\varepsilon}$, $\boldsymbol{\kappa}$, $\boldsymbol{\gamma}$, and $\hat{\mathbf{E}}$. More precisely, the identities

$$\varepsilon_{\alpha\beta} = E_{\alpha\beta}^0, \quad \kappa_{\alpha\beta} = E_{\alpha\beta}^1, \quad \gamma_\alpha = 2E_{\alpha 3}^0 \quad (104)$$

hold, identifying the strain distributions of the geometrically exact formulation discussed in this section as a special instance of the more general approach from Section 4.1 (note that the tensor components refer to the same base vectors in both cases). More precisely, the strain measures of the present model can be obtained within the framework of derivation from continuum mechanics by adopting the displacement assumption (89) therein and neglecting strain components that are quadratic with respect to the thickness coordinate θ^3 .

As in the previous section, we intend to find an expression for the strain energy of the shell on the basis of quantities defined on the middle surface only. The remaining step to accomplish this is the definition of stress resultants. In the derivation of a shell formulation from three-dimensional continuum mechanics, these evolve quite naturally from dimensional reduction of the kinematic equations along with the expression for the internal energy in three dimensions. According to the philosophy pursued in the present section, we define *effective stress resultants*

$$\tilde{\mathbf{n}} := \tilde{n}^{\alpha\beta} \mathbf{A}_\alpha \otimes \mathbf{A}_\beta \quad (105)$$

$$\tilde{\mathbf{m}} := \tilde{m}^{\alpha\beta} \mathbf{A}_\alpha \otimes \mathbf{A}_\beta \quad (106)$$

$$\tilde{\mathbf{q}} := \tilde{q}^\alpha \mathbf{A}_\alpha \quad (107)$$

as energetically conjugate quantities to the strain variables, equations (100)–(102). For a detailed derivation and discussion of the underlying concept see Simo and Fox (1989), as well as Simo, Fox and Rifai (1989). These definitions match, in principle, the ones from the previous section, equation (79). However, while definition of the components n_M^{ij} was straightforwardly derived from the three-dimensional equations in the previous section, they are merely postulated within the framework of the present approach.

Simo and Fox (1989) specify the coefficients of the stress resultants for isotropic constitutive relations as

$$\tilde{n}^{\alpha\beta} = \bar{J}^{-1} \frac{Et}{1-\nu^2} H^{\alpha\beta\gamma\delta} \varepsilon_{\gamma\delta} \quad (108)$$

$$\tilde{m}^{\alpha\beta} = \bar{J}^{-1} \frac{Et^3}{12(1-\nu^2)} H^{\alpha\beta\gamma\delta} \kappa_{\gamma\delta} \quad (109)$$

$$\tilde{q}^\alpha = \bar{J}^{-1} \alpha_s Gt A^{\alpha\beta} \gamma_\beta \quad (110)$$

with

$$\bar{J} = \frac{\|\mathbf{a}_1 \times \mathbf{a}_2\|}{\|\mathbf{A}_1 \times \mathbf{A}_2\|},$$

$$H^{\alpha\beta\gamma\delta} = \nu A^{\alpha\beta} A^{\gamma\delta} + \frac{1}{2} (1-\nu) (A^{\alpha\gamma} A^{\beta\delta} + A^{\alpha\delta} A^{\beta\gamma}) \quad (111)$$

The shear correction factor α_s is typically chosen to be $\alpha_s = (5/6)$. A derivation of this value is given in Section 4.4.5. Similar expressions can be obtained for anisotropic material behavior.

Equations (108)–(110) differ in a couple of aspects from the format that emanates from equations (80) and (77). First, the above equations are obtained from the assumption of vanishing transverse normal stresses, implementing corresponding modifications of the stress–strain relationship (see Section (4.4.5) below for details). Second, definition of the components H^{ijkl} of the constitutive tensor relies on the midsurface metric $A^{\alpha\beta}$ instead of G^{ij} . In fact, the stiffness expressions utilized in equations (108)–(110) can be obtained directly from (77) by replacing G^{ij} by A^{ij} in the formulae for C^{ijkl} therein and introducing the aforementioned condition $S^{33} = 0$. As A^{ij} is constant in θ^3 , through-the-thickness integration is accomplished analytically, independent of shell geometry. This means at the same time that information about initial curvature of the shell is neglected in the material law in the present approach, restricting applicability of the formulation to thin shells. Technically, this assumption is identical to assuming $\mathbf{Z} = \mathbf{G}$ in the constitutive law, which is discussed in detail in Section 4.4.4.

The determinant of the inverse Jacobian \bar{J}^{-1} , showing up in the definitions of the components of the stress resultants is merely a matter of definition (it is included here because we wanted to stick as close as possible to the original notation in Simo and Fox (1989)). It cancels later in the energy expression (cf. equation (116) below).

With the abbreviations

$$D_n^{\alpha\beta\gamma\delta} = \frac{Et}{1-\nu^2} H^{\alpha\beta\gamma\delta} \quad (112)$$

$$D_m^{\alpha\beta\gamma\delta} = \frac{Et^3}{12(1-\nu^2)} H^{\alpha\beta\gamma\delta} \quad (113)$$

$$D_q^{\alpha\beta} = \alpha_s Gt A^{\alpha\beta} \quad (114)$$

the relationship between effective stress resultants and strain measures is established as

$$\bar{J}\tilde{n}^{\alpha\beta} = D_n^{\alpha\beta\gamma\delta}\varepsilon_{\gamma\delta}, \quad \bar{J}\tilde{m}^{\alpha\beta} = D_m^{\alpha\beta\gamma\delta}\kappa_{\gamma\delta}, \quad \bar{J}\tilde{q}^\alpha = D_q^{\alpha\beta}\gamma_\beta \quad (115)$$

and the internal virtual work can be written as

$$-\delta\Pi^{\text{int}} = \int_{\Omega^0} \bar{J}(\tilde{n}^{\alpha\beta}\delta\varepsilon_{\alpha\beta} + \tilde{m}^{\alpha\beta}\delta\kappa_{\alpha\beta} + \tilde{q}^\alpha\delta\gamma_\alpha) d\Omega^0 \quad (116)$$

Again, this expression can be obtained from equation (76) by implementing the previously discussed assumptions for displacements, strains, stresses, and constitutive equations (see Section 4.4 for details concerning these model decisions).

4.3 Degenerated solid approach

In contrast to what has been described in Sections 4.1 and 4.2, the concept of degeneration is directly related to the formulation of finite elements, that is, there is no such thing as a shell ‘theory’ based on this concept. Nevertheless, we will see that strong similarities to finite elements based on shell theories exist. In fact, the final finite element result may even be the same although the path of derivation is different, provided the same mechanical and numerical assumptions are chosen.

In rough terms, the idea of developing shell finite elements via degeneration means switching the sequence of dimensional reduction and discretization. Thus, the starting point is a finite element discretization of the

three-dimensional continuum. Shell elements based on the degenerated solid approach are therefore also denoted as continuum-based shell elements. Linear shape functions in thickness direction are used, thus naturally implementing the assumption of cross-sectional areas remaining straight as is typical for shell theories with Kirchhoff–Love or Reissner–Mindlin kinematics. However, in principle also, higher-order functions or even more than one element in thickness direction are possible (see Section 5.1.4).

Following an isoparametric concept, identical shape functions are used for discretization of geometry and displacements within an individual element,

$$\mathbf{X} \approx \mathbf{X}_h = \sum_{K=1}^{N_{\text{nod}}} N^K \left(\frac{1}{2}(1-\zeta)\mathbf{X}_{\text{bot}}^K + \frac{1}{2}(1+\zeta)\mathbf{X}_{\text{top}}^K \right) \quad (117)$$

$$\mathbf{x} \approx \mathbf{x}_h = \sum_{K=1}^{N_{\text{nod}}} N^K \left(\frac{1}{2}(1-\zeta)\mathbf{x}_{\text{bot}}^K + \frac{1}{2}(1+\zeta)\mathbf{x}_{\text{top}}^K \right) \quad (118)$$

$$\begin{aligned} \Rightarrow \mathbf{u} \approx \mathbf{u}^h &= \mathbf{X}^h - \mathbf{x}^h \\ &= \sum_{K=1}^{N_{\text{nod}}} N^K \left(\frac{1}{2}(1-\zeta)\mathbf{u}_{\text{bot}}^K + \frac{1}{2}(1+\zeta)\mathbf{u}_{\text{top}}^K \right) \end{aligned} \quad (119)$$

The upper index h indicates as usual the field variables after discretization. The vectors $\mathbf{X}_{\text{bot}}^K$ and $\mathbf{X}_{\text{top}}^K$ represent position vectors to bottom and top nodes, as illustrated in Figure 6. Similar definitions hold for $\mathbf{x}_{\text{bot}}^K$, $\mathbf{x}_{\text{top}}^K$ as well as $\mathbf{u}_{\text{bot}}^K$ and $\mathbf{u}_{\text{top}}^K$. Further, $N^K(\xi, \eta)$ are two-dimensional

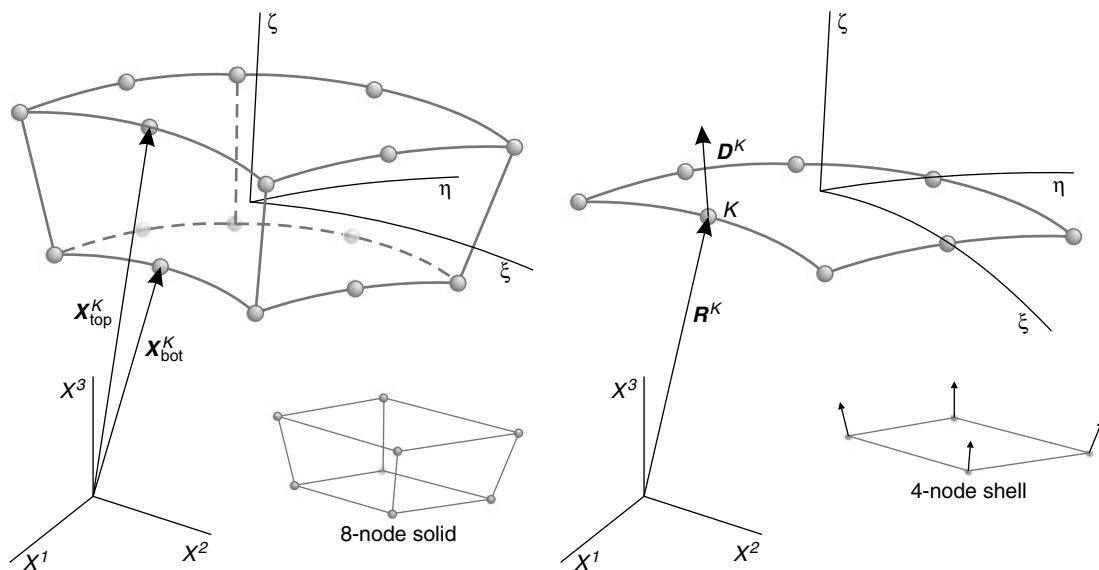


Figure 6. Continuum-based shell elements, degenerated solid approach. A color version of this image is available at <http://www.mrw.interscience.wiley.com/ecm>

shape functions, with ξ and η representing the in-plane coordinates of the shell element; ζ denotes the normalized thickness coordinate. As is customary in finite elements, their range is chosen to be $-1 \leq \{\xi, \eta, \zeta\} \leq 1$.

For instance, for a four-node shell element (see the smaller pictures in Figure 6) we have

$$N^K = \frac{1}{4}(1 + \xi^K \xi)(1 + \eta^K \eta) \quad (120)$$

where ξ^K and η^K are the nodal coordinate values in the parameter space of the element. Replacing these shape functions in one of equations (117–119) recovers the shape functions of the corresponding trilinear element,

$$\begin{aligned} & \frac{1}{4}(1 + \xi^K \xi)(1 + \eta^K \eta) \frac{1}{2}(1 - \zeta) \\ &= \frac{1}{8}(1 + \xi^K \xi)(1 + \eta^K \eta)(1 - \zeta) \\ & \frac{1}{4}(1 + \xi^K \xi)(1 + \eta^K \eta) \frac{1}{2}(1 + \zeta) \\ &= \frac{1}{8}(1 + \xi^K \xi)(1 + \eta^K \eta)(1 + \zeta) \end{aligned} \quad (121)$$

Substituting

$$\mathbf{R}^K = \frac{1}{2}(\mathbf{X}_{\text{top}}^K + \mathbf{X}_{\text{bot}}^K), \quad \mathbf{D}^K = \frac{1}{t^K}(\mathbf{X}_{\text{top}}^K - \mathbf{X}_{\text{bot}}^K) \quad (122)$$

$$\mathbf{r}^K = \frac{1}{2}(\mathbf{x}_{\text{top}}^K + \mathbf{x}_{\text{bot}}^K), \quad \mathbf{d}^K = \frac{1}{t^K}(\mathbf{x}_{\text{top}}^K - \mathbf{x}_{\text{bot}}^K) \quad (123)$$

into equations (117) and (118) yields

$$\mathbf{X}^h = \sum_{K=1}^{N_{\text{nod}}} N^K \left(\mathbf{R}^K + \frac{t^K}{2} \zeta \mathbf{D}^K \right) \quad (124)$$

$$\mathbf{x}^h = \sum_{K=1}^{N_{\text{nod}}} N^K \left(\mathbf{r}^K + \frac{t^K}{2} \zeta \mathbf{d}^K \right) \quad (125)$$

Normalization of \mathbf{D}^K and \mathbf{d}^K via the nodal thicknesses $t^K = \|\mathbf{X}_{\text{top}}^K - \mathbf{X}_{\text{bot}}^K\|$ is not necessary, but is used here to facilitate comparison to finite elements derived from shell theories. Note that equations (124) and (125) establish interpolation of nodal vectors of length $t^K \|\mathbf{D}^K\| = t^K$ instead of interpolating thickness t and directors \mathbf{D} separately, which is not equivalent.

A two-dimensional parameterization of the displacements, based upon quantities defined on the midsurface of the shell, is thus given as

$$\mathbf{u}^h = \sum_{K=1}^{N_{\text{nod}}} N^K \left(\mathbf{R}^K - \mathbf{r}^K + \frac{t^K}{2} \zeta (\mathbf{D}^K - \mathbf{d}^K) \right)$$

$$= \sum_{K=1}^{N_{\text{nod}}} N^K \left(\mathbf{v}^K + \frac{t^K}{2} \zeta \mathbf{w}^K \right) \quad (126)$$

Here, the vector $\mathbf{v}^K = \mathbf{r}^K - \mathbf{R}^K$ represents the displacement of a midsurface node and the so-called *difference vector* $\mathbf{w}^K = \mathbf{d}^K - \mathbf{D}^K$ updates the director vector.

It is noticeable that with the given parameterization, six independent variables are used to describe the deformation at each node, namely, three independent components each for \mathbf{v}^K and \mathbf{w}^K . In comparison to the 5-parameter models described in the previous section, assuming an inextensible director, this 6-parameter formulation naturally includes thickness changes of the shell. This is obviously a result of deriving the parameterization directly from a three-dimensional solid element. In fact, the kinematical content of this formulation is of course identical to that of a solid element with nodes on either surface with a linear displacement field across the thickness. Although this additional feature may seem attractive in the first place, because it potentially enhances the capabilities of the resulting shell elements in the range of thick shells, there are two major reasons why this simple formulation needs additional modifications.

Firstly, and most importantly, the resulting shell element is not asymptotically correct. The reason is that bending cannot be represented properly because of the presence of artificial normal stresses in thickness direction. This phenomenon, sometimes called *thickness locking* or *Poisson thickness locking* in the literature, is explained in more detail in Section 4.4.5. Secondly, conditioning of the corresponding element stiffness matrices is much worse than in conventional 5-parameter shell elements due to the extremely high stiffness in transverse normal direction (Simo, Rifai and Fox, 1990; Wall, Gee and Ramm, 2000).

Possibilities of preserving through-the-thickness stretching within the shell model, thus formulating three-dimensional shell elements are outlined in Section 4.4. In the remainder of this chapter, however, we follow the classical concept of Ahmad, Irons and Zienkiewicz (1968) (see also Ahmad, Irons and Zienkiewicz, 1970) and for arbitrarily large rotations, Ramm (1976, 1977), to derive a 5-parameter shell element on the basis of two fundamental postulates:

1. Transverse normal strains are negligible.
2. Transverse normal stresses are negligible.

The assumptions $E_{33} = 0$ and $S_{33} = 0$, which are actually contradictory for the three-dimensional continuum, require two additional modifications, one ensuring inextensibility of the director and the other one modifying the material equations. It is worth a remark that this contradiction is

not an exclusive quality of the degenerated solid approach but also appears within classical plate and shell theory (Timoshenko and Woinowsky-Krieger, 1959).

The first modification implements the additional condition

$$\|\mathbf{D}^K\| = \|\mathbf{d}^K\| = \|\mathbf{D}^K + \mathbf{w}^K\| \quad (127)$$

for the difference vector \mathbf{w}^K . It can be realized quite naturally by defining

$$\mathbf{w}^K = \mathbf{d}^K - \mathbf{D}^K = \mathbf{\Lambda}^K \cdot \mathbf{D}^K - \mathbf{D}^K = (\mathbf{\Lambda}^K - \mathbf{G}) \cdot \mathbf{D}^K \quad (128)$$

where $\mathbf{\Lambda}^K \in \mathcal{S}_D^2$ is the rotation tensor introduced in the previous section (see also Section 5.3) at node K . To sum up, displacements and deformations of a shell element are given by

$$\mathbf{u}^h = \sum_{K=1}^{N_{\text{nod}}} N^K \left(\mathbf{v}^K + \frac{t^K}{2} \zeta (\mathbf{\Lambda}^K - \mathbf{G}) \cdot \mathbf{D}^K \right) \quad (129)$$

As $\mathbf{\Lambda}^K$ involves only two independent parameters, we arrive at a 5-parameter formulation. The second modification, affecting the formulation of the material law and valid for arbitrary anisotropic materials, is elaborated in Section 4.4.5. For the time being, we are only using the result in the form of a modified three-dimensional material law for the isotropic case (cf. equation (46))

$$\bar{\mathbf{C}}_h^{ijkl} = \bar{\lambda} G_h^{ij} G_h^{kl} + \mu (G_h^{ik} G_h^{jl} + G_h^{il} G_h^{jk}) \quad (130)$$

with

$$\bar{\lambda} = \frac{2\lambda\mu}{\lambda + 2\mu} \quad (131)$$

see also Sokolnikoff (1956). Applying equations (130) and (131) instead of (45) and (46) effectively implements the effect of the second assumption, $S^{33} = 0$, on S^{11} and S^{22} , as well as the normal strain components. In other words, it takes away the artificial constraint that comes along with condition (127), leading to thickness locking. Note that in equation (130), the ‘transverse’ direction is not specified, that is, when computing a three-dimensional stress state from a given strain distribution by means of $\bar{\mathbf{C}}_h = \bar{\mathbf{C}}_h^{ijkl} \mathbf{G}_i^h \otimes \mathbf{G}_j^h \otimes \mathbf{G}_k^h \otimes \mathbf{G}_l^h$, the transverse normal stress component (e.g. S_h^{33}) will in general turn out to be nonzero. However, the plane-stress condition is effectively included in the computation of the internal energy (equation (151) below) because the energetically conjugate strain component is identically zero. The often used notion ‘plane-stress’ condition is strictly speaking not correct since transverse shear stresses are present as well.

In a practical finite element implementation, it is customary to use Voigt notation, placing strain and stress components in column vectors. Using equation (130) along with a stress vector that does not take into account transverse normal stresses effectively implements the necessary conditions to obtain an asymptotically correct model.

In order to compare with the developments in Sections 4.1 and 4.2, we express strains in a curvilinear coordinate system $\theta^1, \theta^2, \theta^3$, which we identify with the element coordinate system $\xi, \eta, (t^K/2)\zeta$. Discretized covariant base vectors in the reference and current configurations are obtained in the standard manner as

$$\begin{aligned} \mathbf{A}_\alpha^h &= \mathbf{X}_{,\alpha}^h|_{\theta^3=0} = \mathbf{R}_{,\alpha}^h = \sum_{K=1}^{N_{\text{nod}}} N_{,\alpha}^K \mathbf{R}^K, \\ \mathbf{A}_3^h &= \mathbf{X}_{,3}^h|_{\theta^3=0} = \sum_{K=1}^{N_{\text{nod}}} N^K \mathbf{D}^K \end{aligned} \quad (132)$$

$$\begin{aligned} \mathbf{a}_\alpha^h &= \mathbf{x}_{,\alpha}^h|_{\theta^3=0} = \mathbf{r}_{,\alpha}^h = \sum_{K=1}^{N_{\text{nod}}} N_{,\alpha}^K \mathbf{r}^K, \\ \mathbf{a}_3^h &= \mathbf{x}_{,3}^h|_{\theta^3=0} = \sum_{K=1}^{N_{\text{nod}}} N^K \mathbf{d}^K \end{aligned} \quad (133)$$

Along the same lines, we compute the first and second fundamental forms in the reference configuration,

$$\mathbf{A}_{ij}^h = \mathbf{A}_i^h \cdot \mathbf{A}_j^h, \quad \mathbf{B}_{\alpha\beta}^h = \frac{1}{2} (\mathbf{A}_\alpha^h \cdot \mathbf{A}_{3,\beta}^h + \mathbf{A}_\beta^h \cdot \mathbf{A}_{3,\alpha}^h) \quad (134)$$

and the current configuration

$$\mathbf{a}_{ij}^h = \mathbf{a}_i^h \cdot \mathbf{a}_j^h, \quad \mathbf{b}_{\alpha\beta}^h = \frac{1}{2} (\mathbf{a}_\alpha^h \cdot \mathbf{a}_{3,\beta}^h + \mathbf{a}_\beta^h \cdot \mathbf{a}_{3,\alpha}^h) \quad (135)$$

respectively. The corresponding quantities in shell space are given by

$$\mathbf{G}_\alpha^h = \mathbf{X}_{,\alpha}^h = \mathbf{A}_\alpha^h + \theta^3 \mathbf{A}_{3,\alpha}^h = \sum_{K=1}^{N_{\text{nod}}} N_{,\alpha}^K (\mathbf{R}^K + \theta^3 \mathbf{D}^K) \quad (136)$$

$$\mathbf{G}_3^h = \mathbf{X}_{,3}^h = \mathbf{A}_3^h = \sum_{K=1}^{N_{\text{nod}}} N^K \mathbf{D}^K \quad (137)$$

$$\mathbf{g}_\alpha^h = \mathbf{x}_{,\alpha}^h = \mathbf{a}_\alpha^h + \theta^3 \mathbf{a}_{3,\alpha}^h = \sum_{K=1}^{N_{\text{nod}}} N_{,\alpha}^K (\mathbf{r}^K + \theta^3 \mathbf{d}^K) \quad (138)$$

$$\mathbf{g}_3^h = \mathbf{x}_{,3}^h = \mathbf{a}_3^h = \sum_{K=1}^{N_{\text{nod}}} N^K \mathbf{d}^K \quad (139)$$

$$\mathbf{G}_{ij}^h = \mathbf{G}_i^h \cdot \mathbf{G}_j^h, \quad \mathbf{g}_{ij}^h = \mathbf{g}_i^h \cdot \mathbf{g}_j^h \quad (140)$$

Computation of the corresponding contravariant quantities is straightforwardly carried out utilizing the same equations as in the continuous case.

We obtain for the discretized, three-dimensional strain tensor

$$\mathbf{E}^h = \frac{1}{2}(\mathbf{g}_{ij}^h - \mathbf{G}_{ij}^h)\mathbf{G}_h^i \otimes \mathbf{G}_h^j = \mathbf{Z}_h^T \cdot \hat{\mathbf{E}}^h \cdot \mathbf{Z}_h \quad (141)$$

$$\hat{\mathbf{E}}^h = E_{ij}^h \mathbf{A}_h^i \otimes \mathbf{A}_h^j, \quad \mathbf{Z}_h = \mathbf{G}_h^i \otimes \mathbf{A}_h^i \quad (142)$$

$$E_{\alpha\beta}^h = \frac{1}{2}[(a_{\alpha\beta}^h - A_{\alpha\beta}^h) + \theta^3(b_{\alpha\beta}^h - B_{\alpha\beta}^h) + (\theta^3)^2(\mathbf{a}_{3,\alpha}^h \cdot \mathbf{a}_{3,\beta}^h - \mathbf{A}_{3,\alpha}^h \cdot \mathbf{A}_{3,\beta}^h)] \quad (143)$$

$$E_{\alpha 3}^h = \frac{1}{2}[(a_{\alpha 3}^h - A_{\alpha 3}^h) + \theta^3(\mathbf{a}_3^h \cdot \mathbf{a}_{3,\alpha}^h - \mathbf{A}_3^h \cdot \mathbf{A}_{3,\alpha}^h)] = E_{3\alpha}^h \quad (144)$$

$$E_{33}^h = 0 \quad (145)$$

A substantial difference in comparison to equation (98), obtained in the course of the direct approach, comes into the picture due to the fact that the linear part of the transverse shear strains with respect to the thickness coordinate θ^3 is in general nonzero. The reason is the interpolation of nodal directors \mathbf{D}^K , which does not preserve the individual director lengths. Note that this is not an approximation or additional assumption but a direct consequence of straightforwardly applying the degenerated solid approach.

In view of a finite element formulation, however, this is neither an advantage nor a drawback of the degenerated solid approach as compared to finite elements derived from shell theory. It is merely a consequence of switching the sequence of dimensional reduction and discretization. If – for instance in the context of a finite element formulation based on a geometrically exact shell model – an interpolation of the directors is applied without subsequent normalization within the element domain, the same issue comes up (although it may not be taken into account explicitly because the corresponding strain components have been removed beforehand when deriving the governing equations of the underlying shell theory).

Up to here, *discretization* and *modification of the material law* have been accomplished. The mechanical ingredients necessary for a correct description of the mechanical behavior of shells, particularly in the thin limit, are thus provided and it is possible to directly formulate finite elements on the basis of the given equations. Computation of the stiffness matrix then involves (numerical) integration of the virtual internal energy in three dimensions. This procedure is sometimes classified with the term *explicit thickness integration* in the literature.

It is, however, usually more efficient to perform a dimensional reduction for the internal energy expression as well. As in Section 4.1, this step involves definition of strain

variables and energetically conjugate stress resultants, along with a corresponding material law.

From equations (143)–(145), we obtain for the strain variables

$$E_{\alpha\beta}^{0h} = \frac{1}{2}(a_{\alpha\beta}^h - A_{\alpha\beta}^h), \quad E_{\alpha 3}^{0h} = \frac{1}{2}(a_{\alpha 3}^h - A_{\alpha 3}^h) = E_{3\alpha}^{0h} \quad (146)$$

$$E_{\alpha\beta}^{1h} = b_{\alpha\beta}^h - B_{\alpha\beta}^h,$$

$$E_{\alpha 3}^{1h} = \frac{1}{2}(\mathbf{a}_3^h \cdot \mathbf{a}_{3,\alpha}^h - \mathbf{A}_3^h \cdot \mathbf{A}_{3,\alpha}^h) = E_{3\alpha}^{1h} \quad (147)$$

$$E_{\alpha\beta}^{2h} = \frac{1}{2}(\mathbf{a}_{3,\alpha}^h \cdot \mathbf{a}_{3,\beta}^h - \mathbf{A}_{3,\alpha}^h \cdot \mathbf{A}_{3,\beta}^h)$$

$$E_{\alpha 3}^{2h} = 0 = E_{3\alpha}^{2h} \quad (148)$$

$$E_{33}^{0h} = E_{33}^{1h} = E_{33}^{2h} = 0 \quad (149)$$

such that

$$E_{ij}^h = \frac{1}{2}[E_{ij}^{0h} + \theta^3 E_{ij}^{1h} + (\theta^3)^2 E_{ij}^{2h}] \quad (150)$$

The discretized internal virtual work reads

$$-\delta \Pi^{\text{int}} \approx -\delta \Pi_h^{\text{int}} = \int_{\Omega_h^0} \int_{-(t/2)}^{t/2} E_{ij}^h \bar{C}_h^{ijkl} \delta E_{kl}^h \mathbf{Z}_h^h d\theta^3 d\Omega_h^0 \quad (151)$$

representing the approximation of equation (72) after introducing the modified material law defined above. The approximation of the shell shifter is

$$\mathbf{Z}_h := \mathbf{G}_h^i \otimes \mathbf{A}_h^i \rightarrow \mathbf{Z}_h = \text{Det}(\mathbf{Z}_h^{-1}) \quad (152)$$

Along the lines of a conventional 5-parameter model, we omit

1. strain terms that are quadratic in the thickness coordinate θ^3 and
2. the linear part of the transverse shear strains

ending up with

$$\begin{aligned} -\delta \Pi_h^{\text{int}} = & \int_{\Omega_h^0} \int_{-(t/2)}^{t/2} (E_{\alpha\beta}^{0h} + \theta^3 E_{\alpha\beta}^{1h}) \bar{C}_h^{\alpha\beta\gamma\delta} (\delta E_{\gamma\delta}^{0h} \\ & + \theta^3 \delta E_{\gamma\delta}^{1h}) \mathbf{Z}_h^h d\theta^3 d\Omega_h^0 \\ & + \int_{\Omega_h^0} \int_{-(t/2)}^{t/2} [(E_{\alpha\beta}^{0h} + \theta^3 E_{\alpha\beta}^{1h}) \bar{C}_h^{\alpha\beta\gamma 3} \delta E_{\gamma 3}^{0h} \\ & + E_{3\alpha}^{0h} \bar{C}_h^{\alpha 3\gamma\delta} (\delta E_{\gamma\delta}^{0h} + \theta^3 \delta E_{\gamma\delta}^{1h})] \mathbf{Z}_h^h d\theta^3 d\Omega_h^0 \\ & + \int_{\Omega_h^0} \int_{-(t/2)}^{t/2} (E_{3\alpha}^{0h} \bar{C}_h^{\alpha 3\gamma 3} \delta E_{\gamma 3}^{0h}) \mathbf{Z}_h^h d\theta^3 d\Omega_h^0 \end{aligned} \quad (153)$$

Since the strain variables are functions of the in-plane coordinates ξ and η only, we can concentrate through-the-thickness integration on the components of the material

matrix,

$$\begin{aligned} D_{0_h}^{\alpha\beta\gamma\delta} &= \int_{-(t/2)}^{t/2} \bar{C}_h^{\alpha\beta\gamma\delta} Z^h d\theta^3, \\ D_{0_h}^{\alpha\beta\gamma 3} &= \int_{-(t/2)}^{t/2} \bar{C}_h^{\alpha\beta\gamma 3} Z^h d\theta^3 \\ D_{0_h}^{\alpha 3\gamma 3} &= \int_{-(t/2)}^{t/2} \bar{C}_h^{\alpha 3\gamma 3} Z^h d\theta^3 \end{aligned} \quad (154)$$

$$\begin{aligned} D_{1_h}^{\alpha\beta\gamma\delta} &= \int_{-(t/2)}^{t/2} \theta^3 \bar{C}_h^{\alpha\beta\gamma\delta} Z^h d\theta^3 \\ D_{1_h}^{\alpha\beta\gamma 3} &= \int_{-(t/2)}^{t/2} \theta^3 \bar{C}_h^{\alpha\beta\gamma 3} Z^h d\theta^3 \end{aligned} \quad (155)$$

$$D_{2_h}^{\alpha\beta\gamma\delta} = \int_{-(t/2)}^{t/2} (\theta^3)^2 \bar{C}_h^{\alpha\beta\gamma\delta} Z^h d\theta^3 \quad (156)$$

Particularly in the context of the degenerated solid approach, this has been termed *implicit thickness integration*, as opposed to the continuum-typical *explicit thickness integration* in which Gauss quadrature is applied directly to the volume integral. The main advantage of implicit, or preintegration of the material equation is that the number of operations is reduced. In the context of deriving a shell theory along the lines of Section 4.1 or 4.2, this has been a natural ingredient of dimensional reduction.

Equations (154)–(156) exactly correspond to the definition in equation (77) (derivation from three-dimensional continuum), specialized for a 5-parameter model. Equations (112)–(114) (direct approach) can be recovered by assuming $\mathbf{Z}^h = \mathbf{G}^h$ in the definition of the components \bar{C}^{ijkl} and $Z^h = 1$ in the evaluation of the integral, along with introducing a shear correction factor. These similarities again confirm the strong interrelation between the different approaches.

Eventually, we can write the internal virtual work as

$$\begin{aligned} -\delta\Pi_h^{\text{int}} &= \int_{\Omega_h^0} \left[E_{\alpha\beta}^{0h} D_{0_h}^{\alpha\beta\gamma\delta} \delta E_{\alpha\beta}^{0h} + E_{\alpha\beta}^{0h} D_{1_h}^{\alpha\beta\gamma\delta} \delta E_{\gamma\delta}^{1h} \right. \\ &+ E_{\alpha\beta}^{1h} D_{1_h}^{\alpha\beta\gamma\delta} \delta E_{\gamma\delta}^{0h} + E_{\alpha\beta}^{1h} D_{2_h}^{\alpha\beta\gamma\delta} \delta E_{\gamma\delta}^{1h} + E_{\alpha\beta}^{0h} D_{0_h}^{\alpha\beta\gamma 3} \delta E_{\gamma 3}^{0h} \\ &+ E_{3\alpha}^{0h} D_{0_h}^{\alpha 3\gamma\delta} \delta E_{\gamma\delta}^{0h} + E_{\alpha\beta}^{1h} D_{1_h}^{\alpha\beta\gamma 3} \delta E_{\gamma 3}^{0h} + E_{3\alpha}^{1h} D_{1_h}^{\alpha 3\gamma\delta} \delta E_{\gamma\delta}^{0h} \\ &\left. + E_{3\alpha}^{0h} D_{0_h}^{\alpha 3\gamma 3} \delta E_{\gamma 3}^{0h} \right] d\Omega_h^0 \end{aligned} \quad (157)$$

For the sake of completeness, the external virtual work due to a distributed body load \mathbf{b} is given as

$$\begin{aligned} \delta\Pi_h^{\text{ext}} &= \int_{\Omega_h^0} \int_{-(t/2)}^{t/2} \mathbf{b} \cdot \delta\mathbf{u}^h Z^h d\theta^3 d\Omega_h^0 \\ &= \int_{\Omega_h^0} \int_{-(t/2)}^{t/2} \mathbf{b} \cdot \sum_{K=1}^{N_{\text{nod}}} N^K (\delta\mathbf{v}^K + \theta^3 \delta\mathbf{d}^K) Z^h d\theta^3 d\Omega_h^0 \\ &= \int_{\Omega_h^0} \sum_{K=1}^{N_{\text{nod}}} N^K \left(\int_{-(t/2)}^{t/2} \mathbf{b} Z^h d\theta^3 \cdot \delta\mathbf{v}^K \right. \\ &\quad \left. + \int_{-(t/2)}^{t/2} \theta^3 \mathbf{b} Z^h d\theta^3 \cdot \delta\mathbf{d}^K \right) d\Omega_h^0 \end{aligned} \quad (158)$$

from which the consistent nodal forces and moments referring to midsurface displacements and rotation parameters can be obtained. As the specific format depends on the choice of parameterization of $\delta\mathbf{d}^K = (\delta\mathbf{A}^K - \mathbf{G}) \cdot \mathbf{D}^K$, we do without further elaborating this point. It can be remarked, however, that there are no special peculiarities here and the consistent nodal force vector is obtained in the standard manner in the context of a finite element formulation.

Finite elements based on the degenerated solid approach are exactly equivalent to finite elements based on a shell theory if the same model assumptions, parameterization, and interpolation of degrees of freedom are used – an issue that has been discussed for a considerable amount of time (Büchter, 1992; Büchter and Ramm, 1992b). The crucial questions concern assumptions for the shifter \mathbf{Z} associated with preintegration of the material law as well as interpolation of the rotation parameters or the director, respectively.